



# Asymmetry of two types of ENSO in the transition between the East Asian winter monsoon and the ensuing summer monsoon

Jian Shi<sup>1</sup> · Weihong Qian<sup>1</sup>

Received: 23 August 2017 / Accepted: 29 January 2018 / Published online: 27 February 2018  
© Springer-Verlag GmbH Germany, part of Springer Nature 2018

## Abstract

This study investigates the transition from East Asian winter monsoon (EAWM) to following summer monsoon (EASM) under two types of El Niño and La Niña events. A robust out-of-phase transition from weak EAWM to strong EASM is related to El Niño events, which is more distinct in eastern Pacific (EP) El Niño than that in central Pacific (CP) El Niño due to the stronger and wider western North Pacific (WNP) anticyclone (WNPAC) as a persistent atmospheric bridge. The WNPAC differences result from the combined impacts of the warming over northern Indian Ocean (NIO) remotely, the dipolar sea surface temperature (SST) anomalies and the anomalous sinking motion over WNP locally. In terms of La Niña, the out-of-phase strong EAWM to weak EASM transition exists only for CP La Niña. Moreover, this connection is weaker compared to that for El Niño events because of a weaker WNP cyclone (WNPC). Conversely, when EP La Niña occurs, an in-phase transition is detected with a strong EAWM evolving into a strong EASM due to the emergence of WNPAC in summer. For CP and EP La Niña, the cooling SST anomalies over NIO and WNP play opposite roles in affecting WNP summertime circulation anomalies. Observational and model results suggest that the WNPC (WNPAC) is dominated by remote (local) cooling in NIO (WNP) in the summer following CP (EP) La Niña. In addition, the local rising (sinking) flow also contributes to the WNPC (WNPAC) associated with CP (EP) La Niña.

**Keywords** El Niño · La Niña · East Asian winter monsoon (EAWM) · East Asian summer monsoon (EASM) · Western North Pacific anticyclone (WNPAC) · Western North Pacific cyclone (WNPC)

## 1 Introduction

Located in the most prominent monsoon domain, the East Asia experiences a seasonal reversal of the prevailing winds (Lau and Li 1984; Huang et al. 2003). In boreal summer, the southerly flow brings abundant water vapor from the Indian Ocean (IO) and tropical western Pacific (WP) to eastern China, Korean Peninsula, and Japan, which constitute the major Meiyu–Changma–Baiu rainbelt over the East Asia (Tao and Chen 1987; Ding 1994; Chen et al. 2009). The East Asian summer monsoon (EASM) displays large interannual variability, and it can cause devastating natural disasters, such as the severe floods over Yangtze River valley (YRV) in the summer of 1998 (Huang et al. 2003, 2007), the grievous

summer droughts in Chongqing in 2006 (Peng et al. 2007; Wang and Zhang 2008), and the heat waves in eastern China in 2013 (Sun et al. 2014; Chen et al. 2017). Although many efforts have been made to reveal the features of EASM (Lau et al. 1988; Ding 1992; Zhou et al. 2005; Trenberth et al. 2006), the research and prediction of EASM are still a crucial issue in climate fields.

The variability of EASM is affected by not only internal atmospheric variability but also external forcing, such as sea surface temperature (SST), snow cover, soil moisture, and the heating condition over Tibetan Plateau (Charney and Shukla 1981; Lau 1992; Wu and Ni 1997; Huang et al. 2003). Among those factors, the East Asian winter monsoon (EAWM) is a vital indicator. Sun and Sun (1994) reported that the summertime flood/drought along the Yangtze–Huaihe River valley is closely associated with the preceding winter circulation anomalies over East Asia. However, this EAWM-EASM relationship is not statistically significant, especially in terms of precipitation. Using both statistical analyses and numerical simulations, Yan et al.

✉ Weihong Qian  
qianwh@pku.edu.cn

<sup>1</sup> Department of Atmospheric and Oceanic Sciences, School of Physics, Peking University, No. 209 Chengfu Road, Haidian District, Beijing 100871, China

(2011) pointed that a strong EAWM leads to a strong EASM in the following summer. In general, this transition includes two types: the in-phase transition (strong EAWM and succeeding strong EASM or weak EAWM and succeeding weak EASM) and the out-of-phase transition (strong EAWM and succeeding weak EASM or weak EAWM and succeeding strong EASM) (Sun and Sun 1994, 1995; Yan et al. 2003, 2011; Li et al. 2011; Wang and Wu 2012). In recent years, some studies emphasized the role of El Niño–Southern Oscillation (ENSO) in the link of EAWM and the following EASM (Chen 2002; Chen et al. 2000, 2013; Li et al. 2011). For example, Chen et al. (2013) documented that when El Niño occurs, the anomalous western North Pacific anticyclone (WNPAC) is predominant in winter and can persist into the ensuing summer. The southerly flow in the western part of WNPAC weakens the northerly wind of EAWM and enhances the southerly wind of EASM, acting as the atmospheric bridge of EAWM and EASM. This finding is not consistent with the results of Yan et al. (2011). Moreover, they just used linear regression against Niño-3 index to reveal the role of ENSO in the link of EAWM and the following EASM. They did not distinguish different ENSO phases and types, so the potential asymmetry of ENSO was not included therein. More recently, Xu et al. (2016) investigated this potential asymmetry by separating the impacts of El Niño and La Niña events, but the effects of different ENSO types were still not elucidated. Still and all, the consensus on the EAWM-EASM relationship and the modulation of ENSO has not been reached yet.

On the other hand, as a key factor influencing the EAWM-EASM relationship, ENSO is a complicated ocean–atmosphere coupled phenomenon over the tropical Pacific (e.g. Neelin et al. 1998). The El Niño and La Niña events are asymmetric in amplitude, structure, and temporal evolution (Burgers and Stephenson 1999; Kang and Kug 2002; Jin et al. 2003; An et al. 2005). Actually, the climate response to ENSO exhibits an apparent nonlinearity between the warm and cold phases (Zhang et al. 2014, 2015a). The results of Xu et al. (2016) are exactly the interpretation in the aspect of EAWM–EASM circulation systems. In addition, as evidenced in numerical simulations, the circulation anomalies are not symmetrical even if the prescribed SST anomalies are equal with opposite sign (Hoerling et al. 1997; Kang and Kug 2002). Since the last decade, a new type of El Niño event has attracted great attention with its SST anomalies centered in the tropical central Pacific (CP), which is referred to as the “Dateline El Niño” (Larkin and Harrison 2005), “El Niño Modoki” (Ashok et al. 2007), “CP El Niño” (Yu and Kao 2007), or “warm pool El Niño” (Kug et al. 2009). It differs from the canonical El Niño, whose SST anomalies are centered in the tropical eastern Pacific (EP), in both spatial pattern and climate impacts (e.g. Weng et al. 2007; Yu and Kim 2011; Zhang et al. 2013; Wang and Wang

2014). For ease of comparison, we employ the terms “CP El Niño” and “EP El Niño” to denote the new and canonical El Niño events, respectively. As the bridge of EAWM and EASM, the evolution of WNPAC displays distinct characteristics in location, intensity, and lifetime for the CP and EP El Niño (Yuan et al. 2012). But Yuan et al. (2012) did not classify La Niña events, and they only focused on the SST effects from IO. Furthermore, the existence of the CP La Niña is still controversial. Some studies negated its existence, stating that the center of negative SST anomalies does not shift apparently among La Niña cases (Kug et al. 2009; Ren and Jin 2011). While others held that the CP La Niña can be distinguished from the EP type in terms of the ocean surface currents (Shinoda et al. 2013) and climate influences (Cai and Cowan 2009; Yuan and Yan 2013; Zhang et al. 2015b). In this study, we classify both El Niño and La Niña events to make a comprehensive investigation. Considering the indispensable role of ENSO in the EAWM-EASM relationship (e.g. Chen 2002; Chen et al. 2013), the non-ENSO years are not included and discussed here.

In brief, we particularly address the following questions in this paper. Firstly, how does the EAWM-EASM relationship vary under different ENSO phases and types? Secondly, what role does the WNPAC (or the corresponding cyclone over the WNP associated with La Niña events, abbreviated as WNPC) play in the above relationship? Thirdly, what mechanisms are responsible for the variation and evolution of WNPAC/WNPC? The structure of this paper is as follows. In Sect. 2, we describe the data sets and methods applied in this study. The SST characteristics of CP and EP ENSO, such as their evolutions and distributions, are examined in Sect. 3. Based on the selected CP El Niño, EP El Niño, CP La Niña, and EP La Niña events, we analyze the modulation of ENSO on the EAWM-EASM relationship and the role of WNPAC/WNPC in Sect. 4. The underlying mechanisms for WNPAC/WNPC are investigated in Sect. 5. Finally, the conclusions and discussion are provided in Sect. 6.

## 2 Data and methodology

The atmospheric variables are monthly reanalysis data derived from the National Centers for Environmental Prediction/National Center for Atmospheric Research (NCEP/NCAR) (Kalnay et al. 1996). It has a horizontal resolution of  $2.5^\circ \times 2.5^\circ$  with 17 standard pressure levels vertically. We use zonal wind, meridional wind, and omega (vertical velocity in pressure coordinate) in this study. The monthly SST data are obtained from Hadley Centre Sea Ice and Sea Surface Temperature data set (HadISST) on  $1^\circ$  latitude by  $1^\circ$  longitude grid (Rayner et al. 2003). We focus on the period from 1951 to 2016 in this paper. The anomalies are defined as the deviations from monthly climatology over

1981–2010. Seasonal means are constructed by averaging the data in December–January–February (DJF) for boreal winter, March–April–May (MAM) for boreal spring, and June–July–August (JJA) for boreal summer.

To distinguish and select the CP and EP El Niño events, two Niño indices are used. The first one is the Niño-3 index, which is defined as SST anomalies averaged over the eastern equatorial Pacific ( $5^{\circ}\text{S}$ – $5^{\circ}\text{N}$ ,  $150^{\circ}\text{W}$ – $90^{\circ}\text{W}$ ). The second one is the El Niño Modoki index (EMI) (Ashok et al. 2007), defined as  $EMI = [SSTA]_A - 0.5 \times [SSTA]_B - 0.5 \times [SSTA]_C$ . The items  $[SSTA]_A$ ,  $[SSTA]_B$ , and  $[SSTA]_C$  indicate the SST anomalies averaged over the regions of ( $10^{\circ}\text{S}$ – $10^{\circ}\text{N}$ ,  $165^{\circ}\text{E}$ – $140^{\circ}\text{W}$ ), ( $15^{\circ}\text{S}$ – $5^{\circ}\text{N}$ ,  $110^{\circ}\text{W}$ – $70^{\circ}\text{W}$ ), and ( $10^{\circ}\text{S}$ – $20^{\circ}\text{N}$ ,  $125^{\circ}\text{E}$ – $145^{\circ}\text{E}$ ), respectively. Considering the potential different peaks of CP and EP cases (see Fig. 5 of Ashok et al. 2007), we first sift the potential CP (EP) El Niño events for monthly EMI (Niño-3 index) larger than  $0.5^{\circ}\text{C}$  for more than 5 consecutive months (at most 1 month interruption). Secondly, we exclude the years of 2002 and 2004 because they only peaked in boreal summer and decayed before boreal winter. Thirdly, the cases (1957, 1963, 1965, 1986, 1987, 1991, and 2006) with mixed signals from both CP and EP are removed. Thereinto, the year 1957 indicates the ENSO process from 1957 to 1958. Fourthly, the anomalous SST spatial pattern shows some similarities between CP El Niño and EP La Niña, and the latter sometimes mistakenly falls into the CP El Niño group by EMI (e.g. 1954 and 1967). Then, the anomalous SST spatial pattern of the residual potential El Niño cases is applied individually to confirm their phases and types (figures not shown). Based on the above procedures, five CP El Niño cases (1968, 1977, 1990, 1994, and 2009) and eight EP El Niño cases (1951, 1965, 1969, 1972, 1976, 1982, 1997, and 2015) are identified. Then, in order to select the CP and EP La Niña events more reasonably, we adopt the definition proposed by Zhang et al. (2015b). The first step is to identify all the La Niña events on a threshold of  $-0.5^{\circ}\text{C}$  for DJF-mean SST anomalies over the Niño-3.4 region ( $5^{\circ}\text{S}$ – $5^{\circ}\text{N}$ ,  $170^{\circ}\text{W}$ – $120^{\circ}\text{W}$ ). The Niño-3.4 index combines the signals of both CP and EP ENSO. The second step is to classify these cases as CP (EP) type when SST anomalies west (east) of  $150^{\circ}\text{W}$  are larger during the mature phase of La Niña. We choose eight CP La Niña events (1973, 1975, 1983, 1988, 1998, 2000, 2008, and 2011) and eight EP La Niña events (1954, 1955, 1964, 1967, 1971, 1984, 1995, and 2005). The mixed La Niña events (1970, 1999, 2007, and 2010) with SST anomalies covering both CP and EP will not be investigated in the following study.

The intensity of the EAWM can be estimated by an EAWM index (EAWMI), defined by the meridional wind at 850 hPa averaged over the region ( $20^{\circ}\text{N}$ – $40^{\circ}\text{N}$ ,  $100^{\circ}\text{E}$ – $140^{\circ}\text{E}$ ) (black box in Fig. 1a; Yang et al. 2002). The positive value of EAWMI denotes a weak EAWM and vice

versa (Fig. 1a). Moreover, a generally weak WNPAC appears near the Philippine Islands when a weak EAWM occurs (“A” in Fig. 1a). In terms of the EASM index (EASMI), its representation remains highly controversial. Firstly, to have a thorough understanding of the EASM, the map of climatic JJA-mean 850-hPa winds and precipitation is plotted (Fig. 1b). Southerly winds, mostly southwesterlies, prevail over the eastern China and its surrounding seas. The center of subtropical high at 850 hPa is located over the subtropical NP (Fig. 1b). In the aspect of precipitation, the Meiyu–Changma–Baiu rainbelt stands as the primary rain-bearing system for EASM. According to Wang et al. (2008a, b), the existing indices for EASM are classified into five categories: the zonal thermal contrast, the meridional thermal contrast, the shear vorticity of zonal wind, the southwesterly monsoon, and the South China Sea monsoon. They recommended a simple index defined by Wang and Fan (1999), which demonstrates the best combined skill to reveal the circulation and precipitation results of multivariate Empirical Orthogonal Function (MV-EOF). Moreover, this index highlights the Meiyu–Changma–Baiu rainbelt and fundamentally facilitates real-time monitoring (Wang et al. 2008a, b). Thus, we choose this EASMI defined by Wang and Fan (1999) with a reversed sign to depict the EASM variability. In detail, it is calculated by the 850-hPa zonal wind averaged over ( $22.5^{\circ}\text{N}$ – $32.5^{\circ}\text{N}$ ,  $110^{\circ}\text{E}$ – $140^{\circ}\text{E}$ ) minus that averaged over ( $5^{\circ}\text{N}$ – $15^{\circ}\text{N}$ ,  $90^{\circ}\text{E}$ – $130^{\circ}\text{E}$ ) (black boxes in Fig. 1c). The regression pattern against EASMI suggests that when strong EASM (positive EASMI) occurs, the southwesterly anomalies bring abundant water vapor and arouse more rainfall in YRV, Japan, and Maritime Continent (MC) (Fig. 1c). Less rainfall is observed in the northern Philippines and eastern Indo-China Peninsula (Fig. 1c). Notably, the climatic WNP subtropical high at 850 hPa (Fig. 1b) is located northeastward compared to the anomalous WNPAC (Fig. 1c). When a strong EASM occurs with an anomalous WNPAC, the WNP subtropical high intensifies and shifts westward.

Composite analysis and linear regression are utilized in this study. The significance of statistical results is evaluated with the two-tailed Student’s *t* test. The running correlations are computed with varying windows from 9 to 15 years.

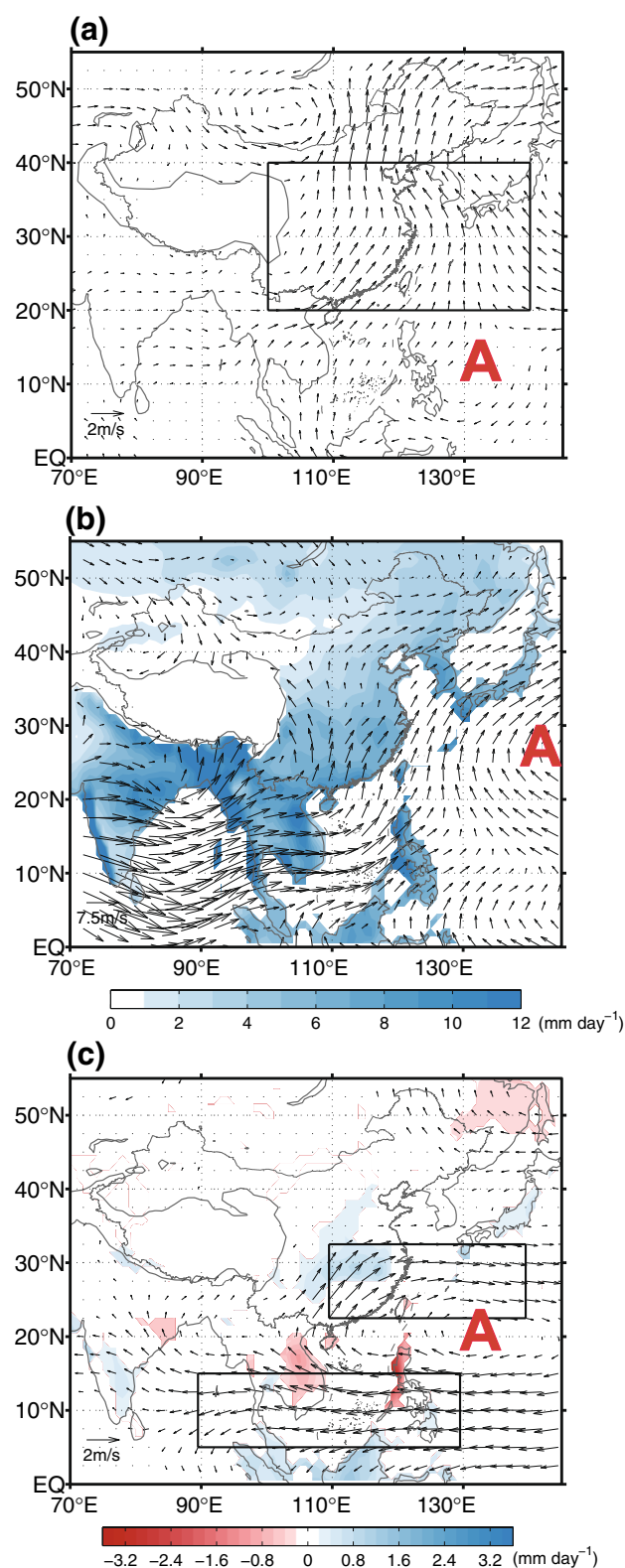
### 3 The asymmetric SST characteristics for two types of ENSO events

First, we compare the horizontal distribution of SST anomalies in the two types of ENSO events (Fig. 2). For the CP El Niño type, the positive SST anomalies are mainly confined in the CP, especially near or slightly east of the dateline (Fig. 2a). The warm center is located west of the  $150^{\circ}\text{W}$ . Negative SST anomalies stretch from the equatorial WP to the subtropical area of the two hemispheres (Fig. 2a). By

**Fig. 1** (a) Regression patterns of DJF-mean 850-hPa wind anomalies (vectors, unit:  $\text{m s}^{-1}$ ) with respect to the simultaneous EAWMI. (b) Climatic pattern of JJA-mean 850-hPa wind (vectors, unit:  $\text{m s}^{-1}$ ) and precipitation (shading, unit:  $\text{mm day}^{-1}$ ). (c) Regression patterns of JJA-mean 850-hPa wind anomalies (vectors, unit:  $\text{m s}^{-1}$ ) and precipitation anomalies (shading, unit:  $\text{mm day}^{-1}$ ) with respect to the simultaneous EASMI. All the plotted vectors and shadings in **a** and **c** reach the 95% confidence level according to a two-tailed Student's *t* test. Black boxes in **a** and **c** indicate the areas to define EAWMI and EASMI, respectively. Letter "A" indicates the anticyclonic anomalies in **a** and **c** as well as the climatic subtropical high over the NP in **b**, respectively. The topography exceeding 3000 ms is outlined and excluded in this study

contrast, the positive SST anomalies are mostly located over the EP for the EP El Niño type, with its center east of  $150^\circ\text{W}$  (Fig. 2b). Moreover, the magnitude of SST anomalies for EP El Niño is much larger than that for the CP El Niño. This distribution of SST anomalies is consistent with previous results of CP and EP El Niño (e.g. Kug et al. 2009; Kim et al. 2011). For La Niña cases, the anomalous SST pattern over tropical Pacific also displays notable differences during boreal winter (Fig. 2c, d). The negative SST center for CP La Niña shifts westward into the equatorial CP west of  $150^\circ\text{W}$  (Fig. 2c). Weak positive SST anomalies in the equatorial WP extend southeastward and northeastward in a horseshoe shape to the subtropical Pacific (Fig. 2c). For EP La Niña, negative SST anomalies cover the equatorial EP with the center far east of  $150^\circ\text{W}$  (Fig. 2d). In addition, the WNP region is also occupied with weak negative SST anomalies (Fig. 2d). The amplitude of the central SST anomalies related to CP La Niña is generally larger than that associated with EP La Niña. This is mostly in agreement with the findings of previous studies (e.g. Dommenges et al. 2013; Frauen et al. 2014; Zhang et al. 2015b; Song et al. 2017). Note that there is nearly no anomalous warming over the tropical WP in the EP La Niña composite (Fig. 2d). Weaker easterlies associated with anomalous Walker Circulation do not penetrate into this region (Fig. 7d), which brings much less warm water and further causes the absence of positive SST anomalies there (Fig. 2d). Based on above distinguishable characteristics, the two types of La Niña cases can be differentiated reasonably under our stipulation.

We further explore the composite evolutions of the equatorial SST anomalies from the developing phase to the decaying phase based on all the above ENSO cases. During the whole lifetime, the position of the central SST anomalies associated with CP ENSO is exactly located to the west of  $150^\circ\text{W}$  and does not show an obvious propagation feature, roughly stationary instead (dots in Fig. 3a, c). In contrast, for both of EP El Niño and EP La Niña, the maximum (or minimum) SST anomalies are mainly located in the equatorial EP, mostly to the east of  $150^\circ\text{W}$  (Fig. 3b, d). It is remarkable that their SST anomalies demonstrate an obvious westward propagation from developing to decaying phases (Fig. 3b, d).



Thereby, above temporal differences between the CP and EP ENSO are conspicuous and consistent with the distinctions in previous studies (Ashok et al. 2007; Kao and Yu 2009; Kug et al. 2009; Feng et al. 2017). Again, not only the two

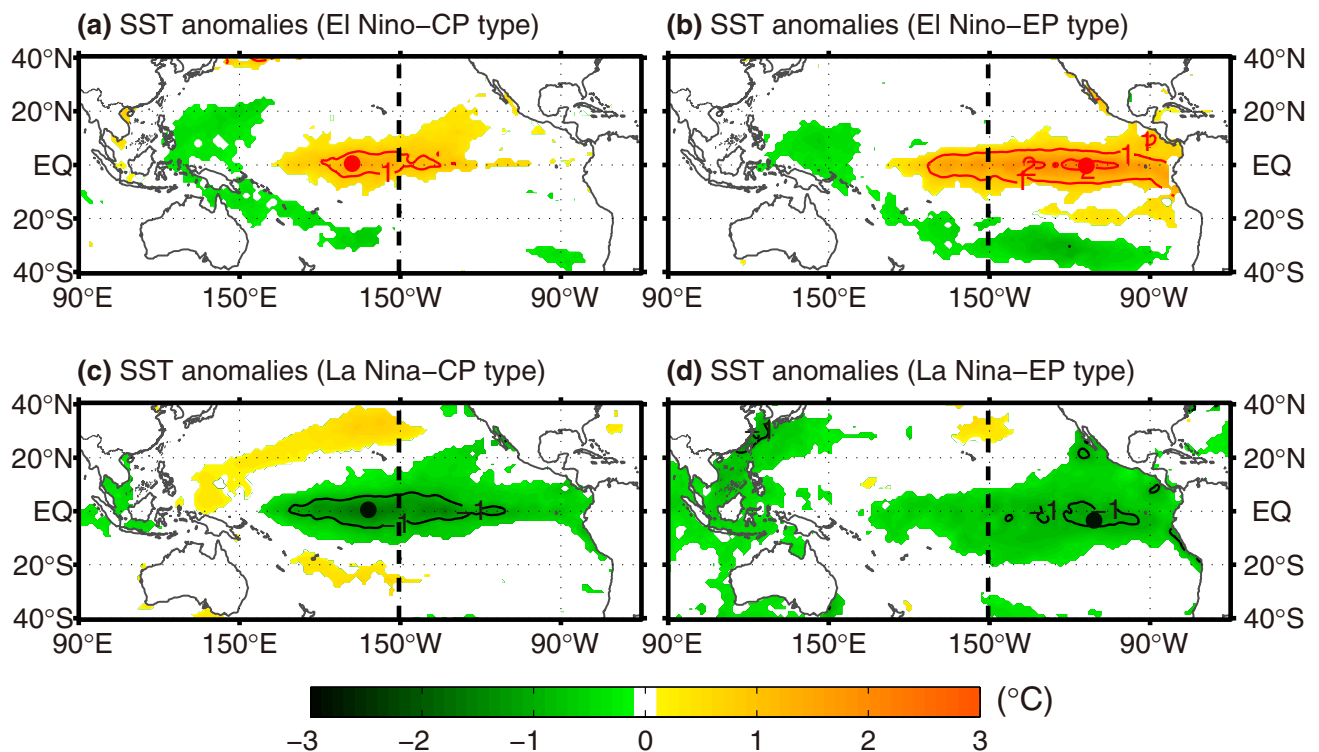


**Fig. 2** The composite DJF-mean SST anomalies (shading with contour, 1 °C interval) for **a** CP El Niño, **b** EP El Niño, **c** CP La Niña, and **d** EP La Niña events. The black-dashed lines denote the longitude of 150°W. The SST anomalies shown here exceed the 95% confidence level

types of El Niño but also La Niña events are well separated through our methods.

Further, the climatology of equatorial SST is calculated to investigate the background of oceanic thermal state (blue line in Fig. 4). It displays high temperature over the WP (i.e. the warm pool) and low temperature over the EP (i.e. the cold tongue). This climatological SST induces different intensities of convection and different sensitivities to convection in the equatorial Pacific. The composite equatorial SST anomalies for CP and EP ENSO are also illustrated in Fig. 4. In terms of El Niño, the differences of two types mainly lie in the central-eastern Pacific. The maximum SST warming (about 1.3 °C) of CP El Niño stands near 170°W (red-solid line in Fig. 4), while that for EP El Niño (around 1.8 °C) occupies the area near 120°W (red-dashed line in Fig. 4). For CP La Niña, the maximum negative SST anomaly is situated near 162°W, with the magnitude about −1.5 °C (black-solid line in Fig. 4). In contrast, the negative SST peak (about −1.1 °C) is located near 120°W for EP La Niña (black-dashed line in Fig. 4). Those are consistent with Figs. 2, 3 and Song et al. (2017).

In short, the spatial distribution, temporal evolution, and propagation features of SST under two ENSO types are notably different. Considering the oceanic state (climatological SST, zonal SST gradient, and total SST) and the nonlinear atmospheric response to oceanic heating, we could speculate

that distinct atmospheric circulation can be detected under different ENSO types and phases.

## 4 Asymmetric modulation of ENSO on EAWM–EASM relationship

### 4.1 Relationship in terms of 850-hPa winds

To reveal the role of ENSO in the transition from EAWM to the following EASM, whether there is asymmetry in the ENSO modulation on EAWM should be perceived first. We calculate the EAWMI series for winters from 1951 to 2016 (Fig. 5a). The EAWM displays large inter-annual variability (Fig. 5a). Then, the ENSO-related part of EAWMI is computed with respect to the synchronous EMI ( $EAWMI_{EMI}$ ; Fig. 5b), Niño-3 index ( $EAWMI_{Niño3}$ ; Fig. 5c), and Niño-3.4 index ( $EAWMI_{Niño3.4}$ ; Fig. 5d), respectively, in order to indicate the synchronous connection between ENSO and EAWM. The correlation coefficients of EAWMI with EMI, Niño-3 index, and Niño-3.4 index are 0.117, 0.364, and 0.363, respectively. The latter two exceed 99% confidence level according to a two-tailed Student's *t* test. As EP ENSO can be well represented by the Niño-3 index, we can conclude that the EP ENSO has a closer and robust relationship with the EAWM. That is,

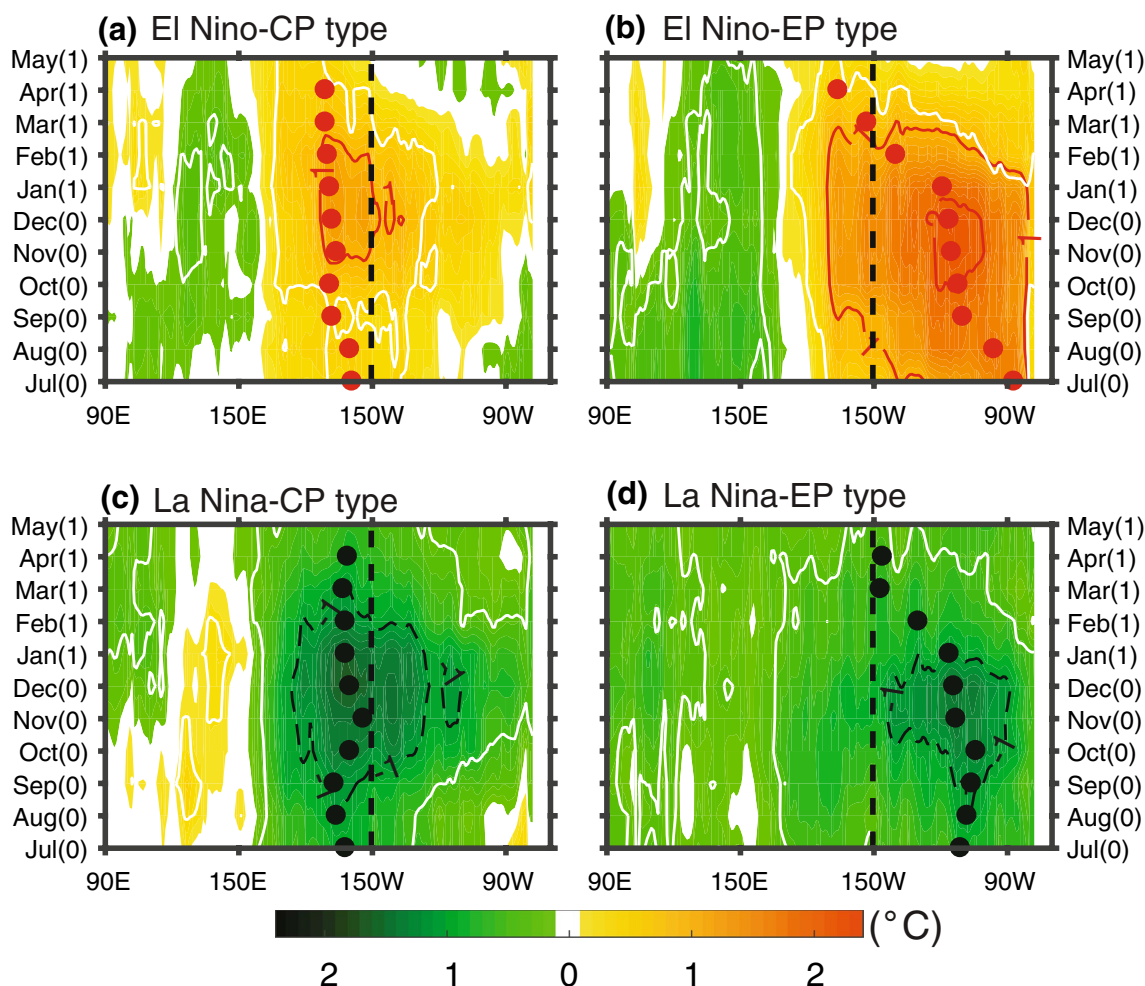


**Fig. 3** The time-longitude section of composite SST anomalies (shading with contour, 1 °C interval) averaged from 5°S to 5°N for **a** CP El Niño, **b** EP El Niño, **c** CP La Niña, and **d** EP La Niña events. Red (black) dots denote the centers of maximum (minimum) SST anomalies for El Niño (La Niña) events. Numbers “0” and “1” in y coord-

inate indicate the developing and decaying years of ENSO events, respectively. The black-dashed lines denote the longitude of 150°W. White contours outline the 95% confidence level based on the two-tailed Student’s *t* test

when EP El Niño (La Niña) occurs, anomalous southerly (northerly) prevails over the East Asia, indicating a weaker (stronger) EAWM. In addition, the above results are consistent with Table 1. It should be noted that the high correlation with Niño-3.4 index may be contributed mostly by the EP ENSO and the inherent association between Niño-3 and Niño-3.4 indices. However, the connection between CP ENSO and EAWM is insignificant from the view of EAWMI<sub>EMI</sub> series and correlation coefficient between EMI and EAWMI (Fig. 5b). Again, the result in Table 1 is an additional corroboration, with almost equivalent probability of strong or weak EAWM after CP ENSO events. Further, taking Niño-3.4 index as an example, it contributes around 13% of the total EAWMI variance, which implies pivotal modulations from other oceanic area or extratropical region.

As proposed in previous studies (e.g. Yuan et al. 2012; Chen et al. 2013), the WNPAC bridges the EAWM and the succeeding EASM. Thus, we elucidate the seasonal transition of East Asian monsoon through the 850 hPa winds, focusing on the seasonal evolution of WNPAC/WNPC (Figs. 6, 7). When CP El Niño occurs, the WNPAC can be observed in the boreal winter (Fig. 6a) and maintained through the following spring (Fig. 6b) and summer (Fig. 6c). The WNPAC in winter can well indicate the weakening EAWM. Then, the WNPAC evolves into two southerly branches in summer and its southern part near the Philippines becomes weak and insignificant (Fig. 6c). In comparison, the WNPAC is much stronger and takes up wider domain in the EP El Niño composite (Fig. 6d–f). Hence, there is a closer connection between EAWM and EASM when EP El Niño arises. Additionally, the WNPAC displays

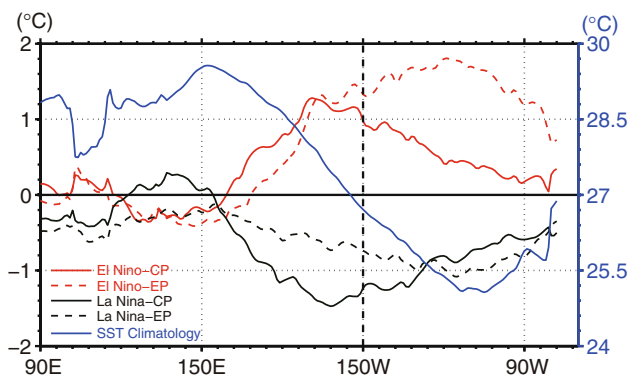


**Fig. 4** Zonal distribution of DJF-mean SST anomalies (unit: °C, the left y-coordinate) in the equatorial (5°S–5°N averaged) Pacific for CP El Niño (red-solid line), EP El Niño (red-dashed line), CP La Niña (black-solid line), and EP La Niña (black-dashed line). The climatological SST (blue line, unit: °C, the right y-coordinate) in the equatorial Pacific. The vertical black-dashed line denotes the longitude of 150°W. The horizontal black-solid line represents zero line for left-side y-coordinate

a zonal-elongated structure under EP El Niño (Fig. 6d–f). Moreover, this is indicative of the out-of-phase weak EAWM to strong EASM transition, mostly in accordance with the previous results (e.g. Yan et al. 2011; Wang and Wu 2012; Chen et al. 2013). Another thing to emphasize is that the anomalous southerly to the northwestern flank of the WNPAC associated with CP El Niño (Fig. 6a) shifts westward over the Eastern China and its surrounding seas in boreal winter compared to that of EP El Niño (Fig. 6d), which may result from the westward location of anomalous SST forcing for CP El Niño (Fig. 2a, b). On the other hand, however, the above relationship does not always hold true under La Niña events (Fig. 7). In the composites of CP La Niña cases (Fig. 7a–c), the strong EAWM is accompanied by the ensuing weak EASM, indicated by the wind anomalies and WNPC. But the WNPC is weaker and smaller than the WNPAC (Fig. 6), and establishes a relatively weaker connection between EAWM and EASM compared to that of WNPAC associated with El Niño events. Differently for EP La Niña cases, the anomalous WNPC is much weaker (Fig. 7d, e) and disappears in summer (Fig. 7f). Note that an anticyclone is located in Mainland China and shifts southeastward into WNPAC over the South China Sea (SCS) in spring (Fig. 7e) and summer (Fig. 7f). Another weak anticyclone is also identified to the east of this WNPAC (Fig. 7f). It implies that the strong EAWM develops into strong EASM following EP La Niña years. After the mature phase of EP La Niña, the circulation pattern in boreal spring (Fig. 7e) and summer (Fig. 7f) shows a complex feature over the East Asia and its surrounding seas, dominant by more than one cyclonic or anticyclonic systems. It suggests that the East

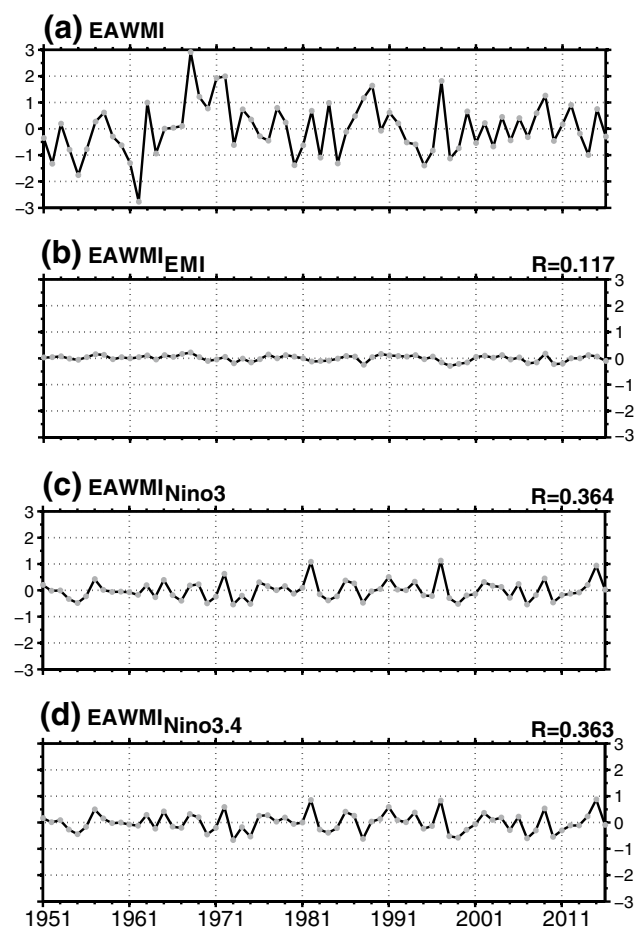


**Fig. 5** The DJF-mean time series (black lines with grey dots) of the normalized **a** EAWMI, and its ENSO-related part by linear regression against **b** EMI ( $EAWMI_{EMI}$ ), **c** Niño-3 index ( $EAWMI_{Niño3}$ ), and **d** Niño-3.4 index ( $EAWMI_{Niño3.4}$ ) for winters from 1951 to 2016. The values in the upper-right location of **b–d** indicate the correlation coefficients of EAWMI with EMI, Niño-3 index, and Niño-3.4 index, respectively

Asian monsoon is affected by many other factors when EP La Niña occurs, partly due to its weak intensity.

To sum up, the out-of-phase EAWM-EASM relationship is more stable and significant when El Niño occurs than that following the La Niña phenomenon, as reported by Xu et al. (2016). In detail, the WNPAC and WNPC exhibit noteworthy asymmetry in intensity, coverage, and location, which is more apparent in boreal summer. The WNPAC is stronger and covers a larger area connecting tropics and mid-latitudes over East Asia and nearby seas, especially in the context of EP El Niño. Inversely, the WNPC is much weaker and then shrinks substantially (associated with CP type) or transforms into WNPAC (associated with EP type) in the decaying year of La Niña, leading to a weaker out-of-phase EAWM-EASM transition or even in-phase EAWM-EASM transition, respectively.

**Table 1** The EAWMI and EASMI following the CP El Niño, EP El Niño, CP La Niña, and EP La Niña events

	CP El Niño	EP El Niño	CP La Niña	EP La Niña
EAWMI	0.457 (5+, 4-)	0.634* (7+, 2-)	- 0.044 (5+, 4-)	- 0.292 (3+, 5-)
EASMI	0.505 (8+, 1-)	0.761* (7+, 2-)	- 0.689* (0+, 9-)	0.051 (3+, 5-)

The values with symbol “\*” exceed the 95% confidence level of the two-tailed Student’s *t* test. The values in the brackets denote the number of occurrence for positive and negative indices, respectively

## 4.2 Relationship in terms of the EAWMI and succeeding EASMI

To further explore the connection between EAWM and the following EASM quantitatively, the correlation coefficients are first computed in terms of EAWMI, EAWMI<sub>EMI</sub>, EAWMI<sub>Niño3</sub>, and EAWMI<sub>Niño3.4</sub> with the succeeding EASMI over the period 1951–2015. They are 0.186, 0.178, 0.413, and 0.402, respectively, with the latter two exceeding 99% confidence level of the two-tailed Student’s *t* test. In other words, when a weak EAWM associated with EP El Niño (positive EAWMI<sub>Niño3</sub>) occurs, a strong EASM (positive EASMI) follows. But a weak EAWM in CP El Niño year or non-ENSO year is not significantly related to a strong EASM afterwards. Thus, we hypothesize that the modulation of moderate-strong EP ENSO is a requisite factor to maintain the out-of-phase transition of EAWM and the following EASM.

The running correlation is also calculated among above indices to reveal the stability of the EAWM-EASM transition with windows of 9, 11, 13, and 15 years (Fig. 8). Again, the out-of-phase EAWM-EASM transition is neither significant nor stable in a general sense (covering both ENSO and non-ENSO years; Fig. 8a), reconfirming the indispensable role of ENSO in the EAWM-EASM relationship. The insignificant EAWM-EASM relationship is also true associated with the CP ENSO (denoted by EMI; Fig. 8b), partly due to its weak linkage with EAWM (Fig. 5b) and the weak intensity of CP El Niño. But the average running correlation against EAWMI<sub>Niño3</sub> is more stable and exceeds the 95% confidence level of the two-tailed Student’s *t* test during most years of the 1979–2001 period (Fig. 8c). This finding proves the importance of EP ENSO (especially EP El Niño; Figs. 6d–f, 7d–f) in maintaining and stabilizing the EAWM-EASM transition. As the Niño-3.4 index largely encompasses the signal of EP ENSO, the similar results against EAWMI<sub>Niño3.4</sub> may result from the dominant effect of EP El Niño (Fig. 8d). Compared with the results in Fig. 5, we conjecture that the modulation of ENSO in the EAWM-EASM transition is significant and robust only on the premise of a significant connection between ENSO and EAWM firstly.

On the other hand, the EAWMI and the following EASMI are calculated based on CP and EP types of ENSO events (Table 1). Statistically, the significant and robust

EAWM-EASM relationship is only detected under EP El Niño. The occurrence of positive EAWMI (7 out of 9) and positive EASMI (7 out of 9) is also dominant. The EASMI under CP La Niña is also significant, but there is no corresponding significant EAWMI before. Not surprisingly, the EAWM–EASM transition is not significant when CP El Niño or EP La Niña occurs. Hence, the EAWM–EASM connection is very complicated in terms of both the value and occurrence of monsoon indices (Table 1).

## 5 Mechanisms for the evolution of WNPAC and WNPC

### 5.1 Mechanisms in terms of oceanic SST effect and vertical motion

As the low-level WNPAC/WNPC is widely regarded as a cardinal system conveying the ENSO impact to East Asia (Zhang et al. 1999; Wang et al. 2000; Wang and Zhang 2002), the underlying mechanisms responsible for the different EAWM–EASM transition during different types of ENSO are elucidated based on the WNPAC/WNPC variations. In terms of the oceanic effects, the Pacific basin can influence the WNPAC/WNPC through a Gill-pattern response (Gill 1980) caused by diabatic heating (Zhang et al. 1996), the local air-sea interaction via wind-evaporation-SST mechanism (Wang et al. 2000; Wang and Zhang 2002), as well as the anomalous vertical motion via the modification of Walker Circulation. Moreover, the IO basin is considered to be more important in affecting the WNPAC/WNPC (Watanabe and Jin 2002; Xie et al. 2009; Wang and Wu 2012), especially the IO basin mode (IOBM; Saji et al. 2006; Du et al. 2009; Deser et al. 2010; Yang et al. 2007) in the maintenance of summer WNPAC/WNPC (Yuan et al. 2012). Wu et al. (2009, 2010) further reported the combined effects of remote SST anomalies over IO and the local SST anomalies.

From the boreal winter (Fig. 9a) to boreal summer (Fig. 9c) of CP El Niño events, the SST anomalies over WNP decay sharply and they are not robust over the northern IO (NIO) either, leading to a relatively weaker intensity of the WNPAC. However, the local SST dipole over the WNP is much stronger following the EP El Niño for the successive winter (Fig. 9d), spring (Fig. 9e), and summer (Fig. 9f).



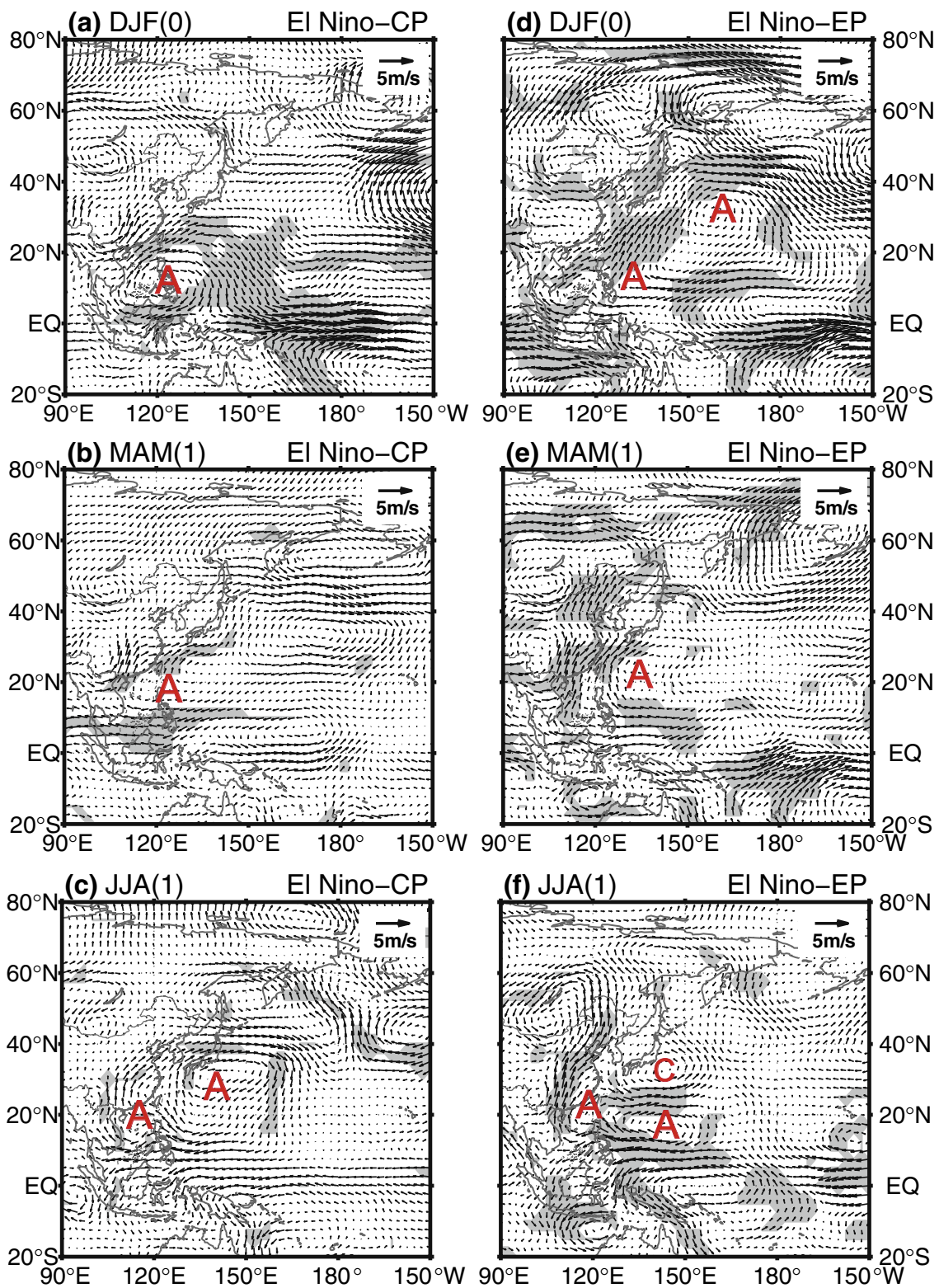


**Fig. 6** Composite distributions of seasonal-mean 850-hPa winds (vector) in **a** DJF(0), **b** MAM(1), and **c** JJA(1) for CP El Niño events. **d–f** Same as **a–c**, but for EP El Niño events. Area with grey shad-

ing reaches the 95% confidence level according to a two-tailed Student's *t* test. The red letters "A" and "C" indicate the anticyclonic and cyclonic anomalies, respectively

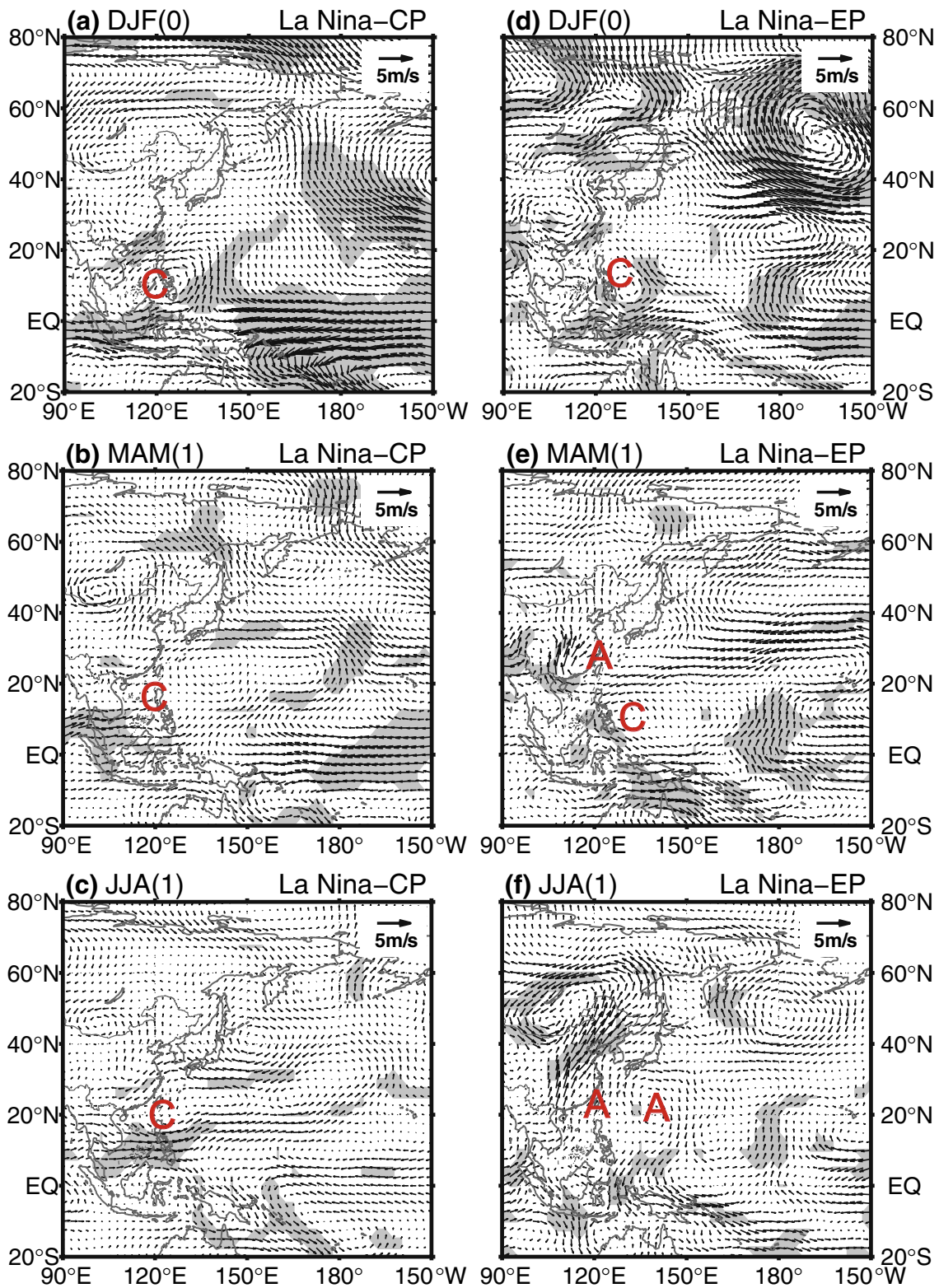
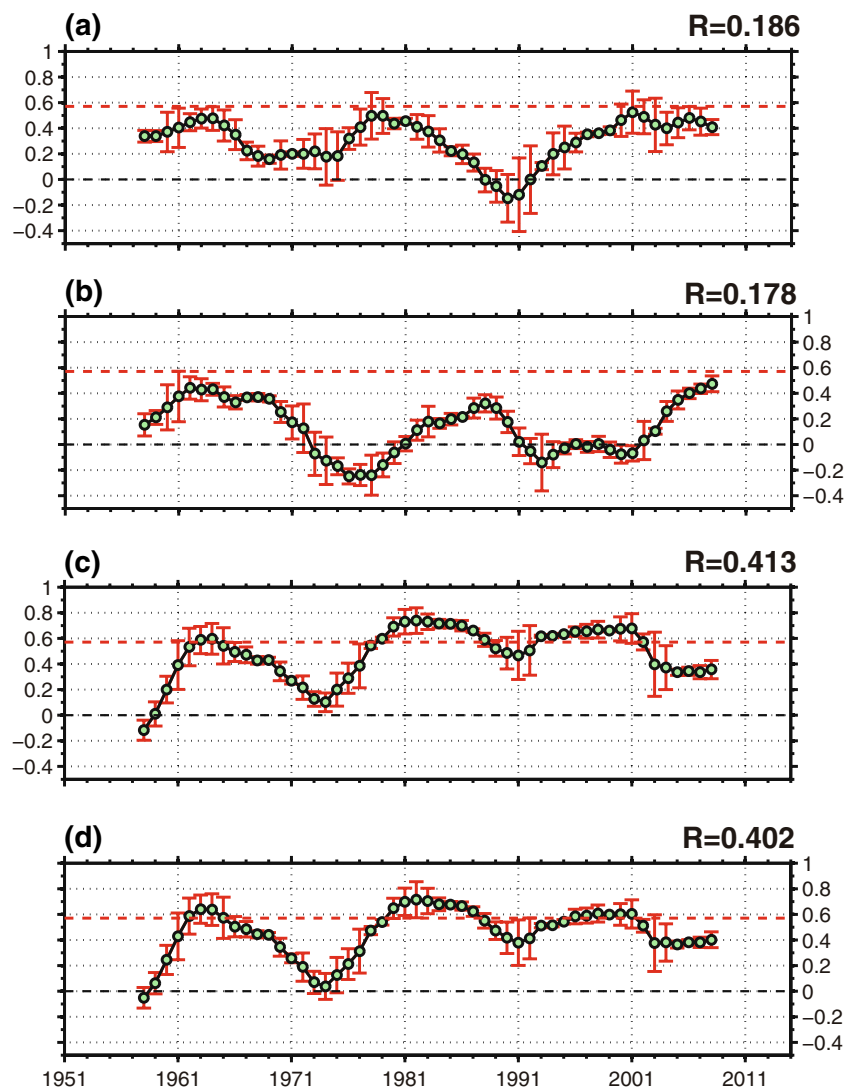


Fig. 7 Same as Fig. 6, but for a–c CP La Niña events and d–f EP La Niña events, respectively

**Fig. 8** The average running correlation coefficients (black lines with green dots; windows of 9, 11, 13, and 15 years; red bar for one standard deviation) between the DJF(0)-mean **a** EAWMI, **b** EAWMI<sub>EMI</sub>, **c** EAWMI<sub>Niño3</sub>, and **d** EAWMI<sub>Niño3.4</sub> and the following JJA(1)-mean EASMI, respectively. The coefficient of 0.58 (red-dashed lines) denotes the 95% confidence level for the average freedom of the four windows. The coefficient of 0 (black-dashed lines) is also highlighted. The values in the upper-right position denote the respective correlation coefficients over the whole period 1951–2015 for EAWM (or 1952–2016 for EASM)



This is important for the continuation of WNPAC. More importantly, the El Niño-induced warming over the NIO acts as the “capacitor” to convey the ENSO effects to the WNPAC and the EASM subsequently, contributing a lot to the persistence of the WNPAC (Xie et al. 2009; Fig. 9d–f). The IO basinwide warming is especially evident in extreme EP El Niño cases, such as in 1982, 1997, and 2015 (figures not shown). Therefore, the anomalous SST following the EP El Niño is more favorable to the maintenance of WNPAC than that following the CP El Niño from the aspects of both remote NIO region and local WNP region. Similar analysis is also conducted for La Niña cases (Fig. 10). Focused on summer (Fig. 10c, f), the basinwide cooling over the NIO is the interpretation of the IOBM, which is largely induced by the tropospheric temperature (TT) mechanism (Chiang and Sobel 2002; Chiang and Lintner 2005). The stronger and significant SST cooling over NIO in the decaying summer of EP La Niña (Fig. 10f) is attributed to a much stronger TT

cooling aloft (figures not shown). The SST cooling over NIO avails the existence of the WNPC, but this favorable condition is largely cancelled by the cooling over the WNP, which goes against the persistence of WNPC by modifying local convection and wind field via a Rossby-wave-type response to the anomalous heating (Hsu and Weng 2001; Wu 2010; Qian and Shi 2017). Thus, this disadvantage leads to the weak WNPC (Fig. 7c) or even the occurrence of WNPAC (Fig. 7f) in the summer of CP and EP La Niña decaying year, respectively. In EP La Niña composite, the magnitude of the negative SST anomalies is equivalent over the WNP and NIO (Fig. 7f). Thus, the local cooling over the WNP exerts more direct and faster impacts on the lower-level circulation anomalies, triggering the summertime WNPAC (Fig. 7f). Furthermore, the complicated circulation pattern (Fig. 7f) is partly caused by the simultaneous wide cooling over both NIO and WNP (Fig. 10f). In a nutshell, the SST anomalies over NIO and WNP play a reversed role in affecting the

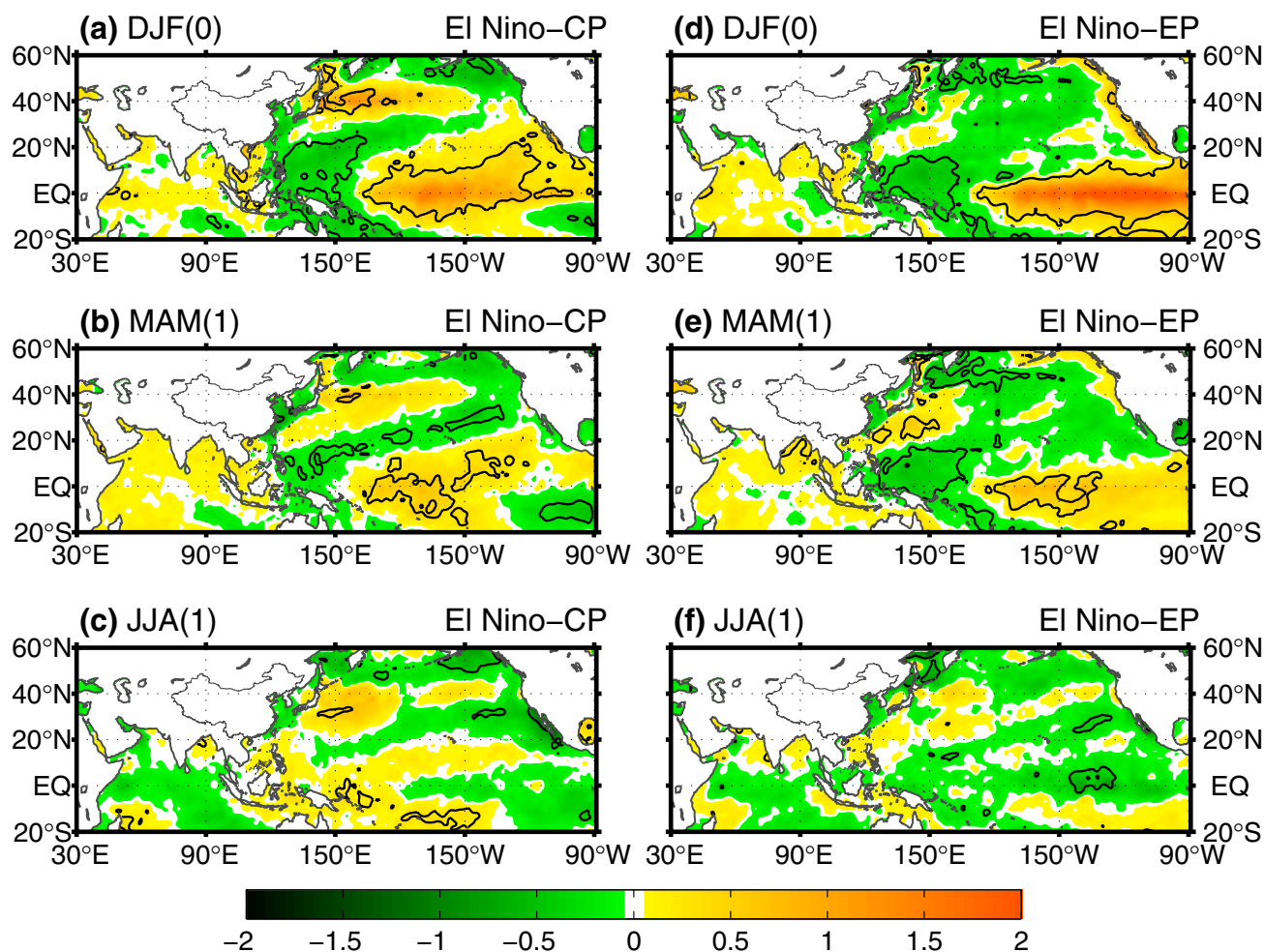


**Fig. 9** Composite evolution of seasonal-mean SST anomalies (shading, unit: °C) in **a** DJF(0), **b** MAM(1), and **c** JJA(1) for CP El Niño events. **d–f** Same as **a–c**, but for EP El Niño events. Black contour

encircles the area reaching the 95% confidence level according to a two-tailed Student's *t* test

WNPC/WNPAC for La Niña composites (Fig. 10c, f), and the net effect under CP La Niña is more conducive to the subsistence of WNPC (Fig. 10c).

In terms of the atmospheric factors, we investigate how the vertical motion affects the evolution of the WNPAC/WNPC (Figs. 11, 12). When CP El Niño happens, there is anomalous sinking over the WNP and anomalous rising over the CP from boreal winter (Fig. 11a) to the following spring (Fig. 11b) and summer (Fig. 11c), which is beneficial to the sustenance of the WNPAC. Actually, this reflects the variation of Walker Circulation due to the anomalous heating over the equatorial CP (Fig. 9a–c). Comparatively, the anomalous subsidence is also detected following the EP El Niño events with stronger intensity and wider coverage (Fig. 11d–f). Note that the location of anomalous rising branch is similar to that in CP El Niño (Fig. 11a–c), which is associated with the threshold of convection and distributions of both climatological SST and SST anomalies (Fig. 4). In

short, the vertical motion under the EP El Niño cases is also more prone to a stronger, wider, and longer-lived WNPAC than that under CP El Niño cases. As for CP La Niña, the ascending anomalies near the Philippines and the descending anomalies near the equatorial dateline are observed evidently in winter (Fig. 12a) and spring (Fig. 12b), attributed to the anomalous cooling over the CP (Fig. 10a, b). In summer, the anomalous ascending flow over the WNP still exists with a slight southwest-northeast orientation (Fig. 12c), which contributes to the persistence of WNPC (Fig. 7c). Nevertheless, this is not the case for EP La Niña (Fig. 12d–f). Because of the weaker intensity and eastward location of EP La Niña events, there are also eastward shifts of both the ascending anomalies to the east of Philippines and descending anomalies over the equatorial EP in winter (Fig. 12d). From spring after the peak phase of EP La Niña, the vertical motion is replaced by anomalous sinking flow over the WNP (Fig. 12e, f), which is consistent with the anticyclonic

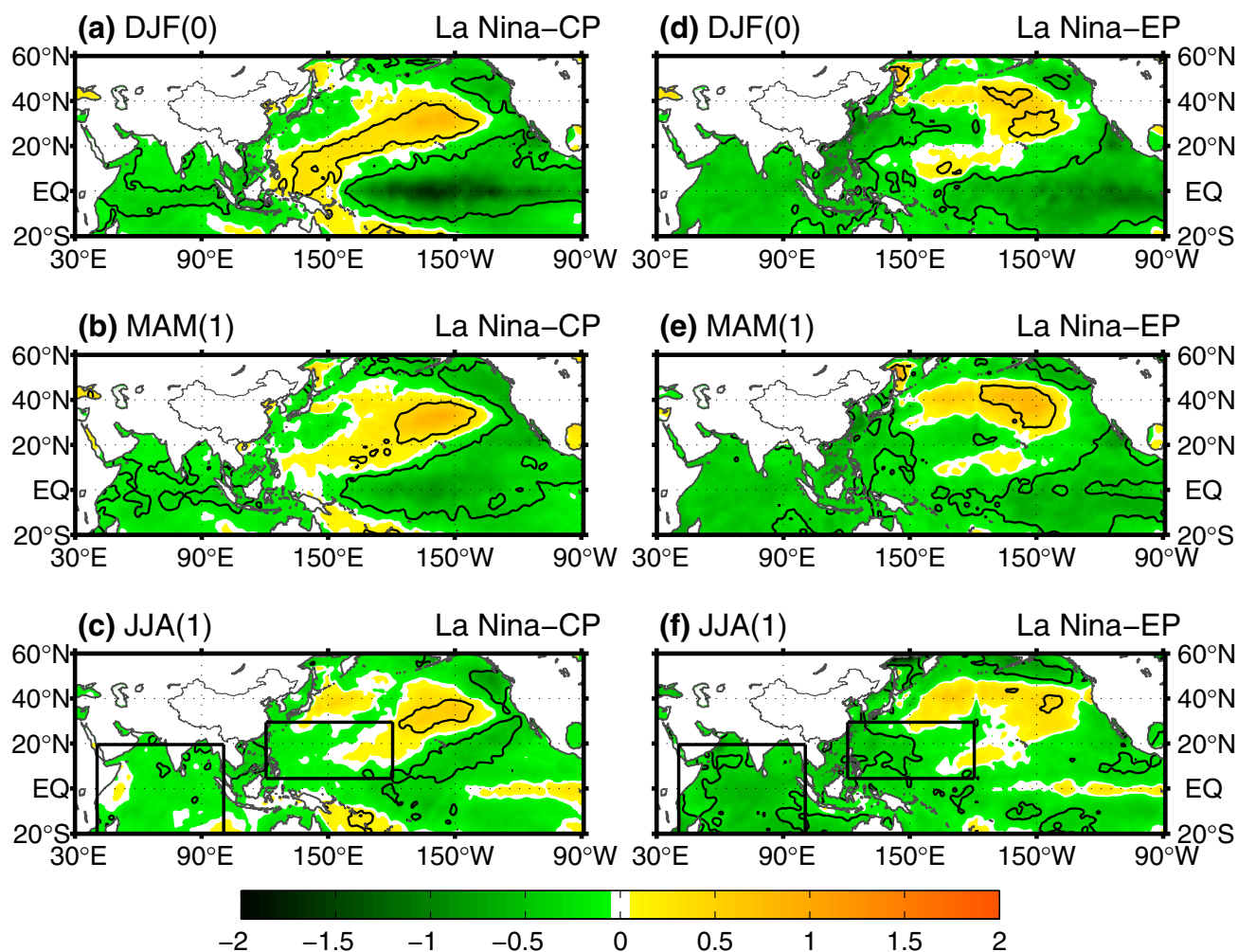


**Fig. 10** Same as Fig. 9, but for **a–c** CP La Niña events and **d–f** EP La Niña events, respectively. The black boxes in **c** and **f** denote the SST forcing area over TIO (20°S–20°N, 40°E–100°E) and WNP (5°N–30°N, 120°E–180°) for CAM5 model runs

anomalies shown in Fig. 7e, f. Hence, the WNPC (WNPAC) related to the CP (EP) La Niña can be well explained from the aspect of atmospheric vertical motion. It is noteworthy that the significant responses of 850-hPa winds (Figs. 6, 7) and 500-hPa vertical motions (Figs. 11, 12) to two types of ENSO are mostly confined over the tropics. However, the counterparts over the East Asia are largely insignificant, except for the EP El Niño composite. As the three historical strongest events are in the EP El Niño group (1982, 1997, and 2015), the significant anomalies over the East Asia are potentially contributed by the extreme EP El Niño cases. Therefore, other factors may be more important or even dominant in the EAWM and EASM variability during the non-extreme (ordinary) ENSO years.

To sum up, the stronger and wider WNPAC in summer following EP El Niño than that following CP El Niño can be mostly attributed to the oceanic effects with a combined favorable SST forcing from remote NIO and local WNP and

the atmospheric effects of vertical motion. While the weak WNPC in the decaying summer of CP La Niña results from the weak net effect of cooling over NIO and WNP as well as the contribution of local rising branch. Following EP La Niña, there is a peculiar WNPAC in summer due to the cooling and anomalous sinking motion over the WNP locally, with a minor opposite impact from the NIO cooling.

## 5.2 Model validation

In this subsection, we perform numerical simulations to validate the above different EAWM-EASM transitions and WNPC/WNPAC evolutions under the two types of La Niña events, focusing on the relative importance of tropical IO (TIO) and WNP. The model verification for El Niño events is not included here. Firstly, the patterns under two types of El Niño events are very distinct and robust (Figs. 6, 9, 11). Secondly, Wu et al. (2010) have conducted numerical

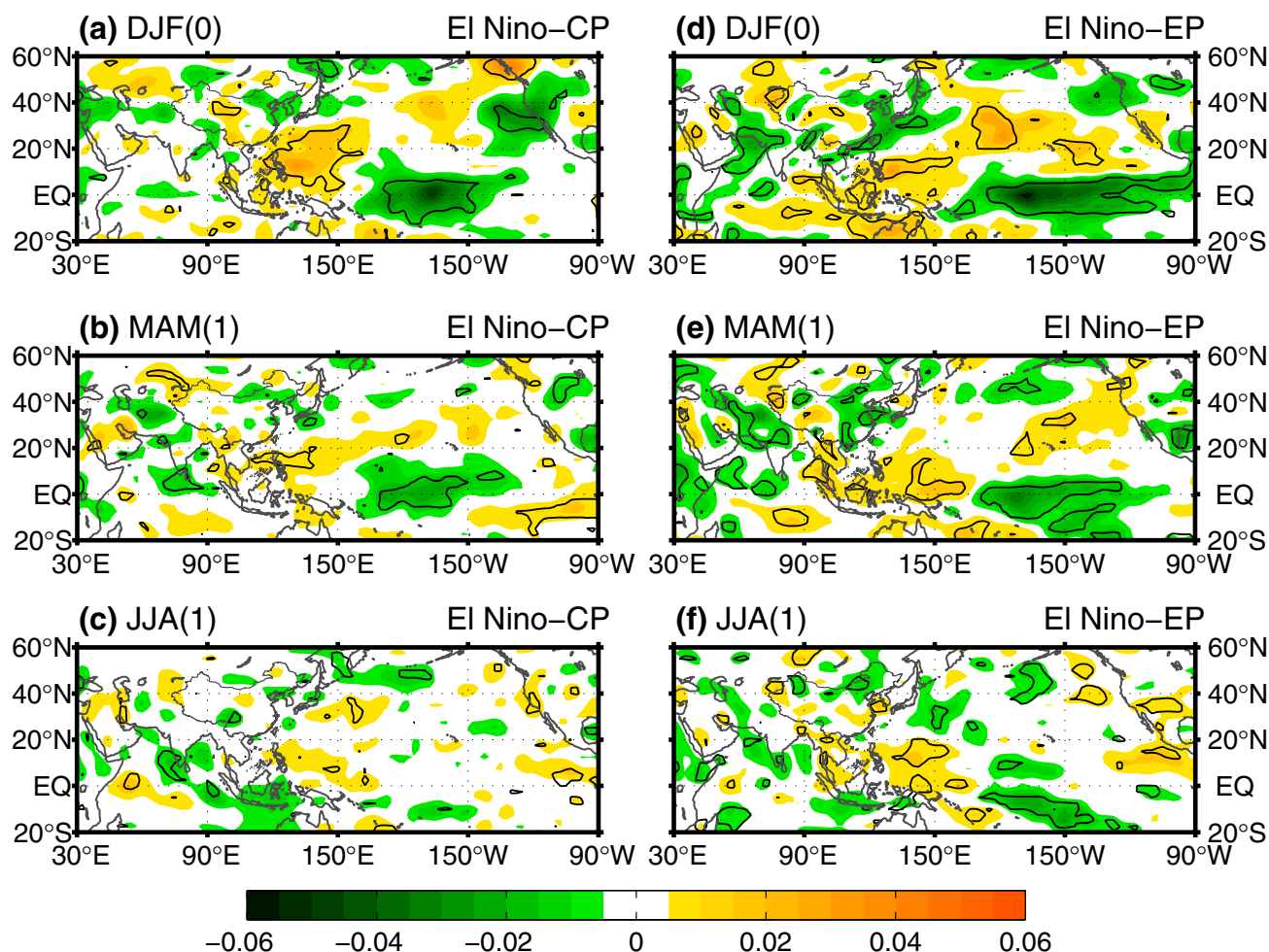


**Fig. 11** Composite distribution of seasonal-mean vertical velocity anomalies (shading, unit:  $\text{Pa s}^{-1}$ ) at 500 hPa in **a** DJF(0), **b** MAM(1), and **c** JJA(1) for CP El Niño events. **d–f** Same as **a–c**, but for EP El

Niño events. Black contour encircles the area reaching the 95% confidence level according to a two-tailed Student's  $t$  test

experiments and demonstrated the relative contributions of the remote TIO and local WNP for the WNPAC during the El Niño decaying summer.

All the experiments in this study are AMIP-type simulations using the version 5.0 of the Community Atmosphere Model (CAM5) developed primarily at NCAR. Five sets of experiments are designed and conducted, including one climatological control experiment (i.e. CTRL) and four sensitivity experiments (i.e. GB run, TIOWNP run, TIO run, and WNP run; see Table 2 for details). The geographic locations for the TIO and WNP domains, similar to those in Fig. 4 of Wu et al. (2010), are illustrated in Fig. 10c, f. The SST data utilized in the model (Hurrell et al. 2008) are merged products based on the version 1 of HadISST (Rayner et al. 2003) and version 2 of the National Oceanic and Atmospheric Administration (NOAA) optimum interpolation SST (Reynolds and Smith 1994). The CTRL run is integrated for 20 years, forced by the monthly climatological SST derived

from the 1981–2000 period. The sensitivity runs are forced by prescribed SST boundary conditions, in which the composite monthly SST anomalies associated with CP (CP-type experiments) and EP La Niña (EP-type experiments) are superimposed to the climatological SST in the global ocean (GB run), both the TIO and WNP (TIOWNP run), the TIO only (TIO run), and the WNP only (WNP run). Note that the SST climatology is prescribed in the regions outside of the anomalous SST forcing area. Each experiment is integrated for 1 year from January to December with ten ensemble members. Considering the close relationship between the climatological circulation and the anomalous circulation over WNP (Chou et al. 2009; Wu et al. 2009), we firstly evaluate the model's performance in the climatology simulation (i.e. CTRL run). The model reproduces the major features of the Asian monsoon in the aspect of wind reversal and advance as well as precipitation variation (figures not shown), laying a foundation to investigate the

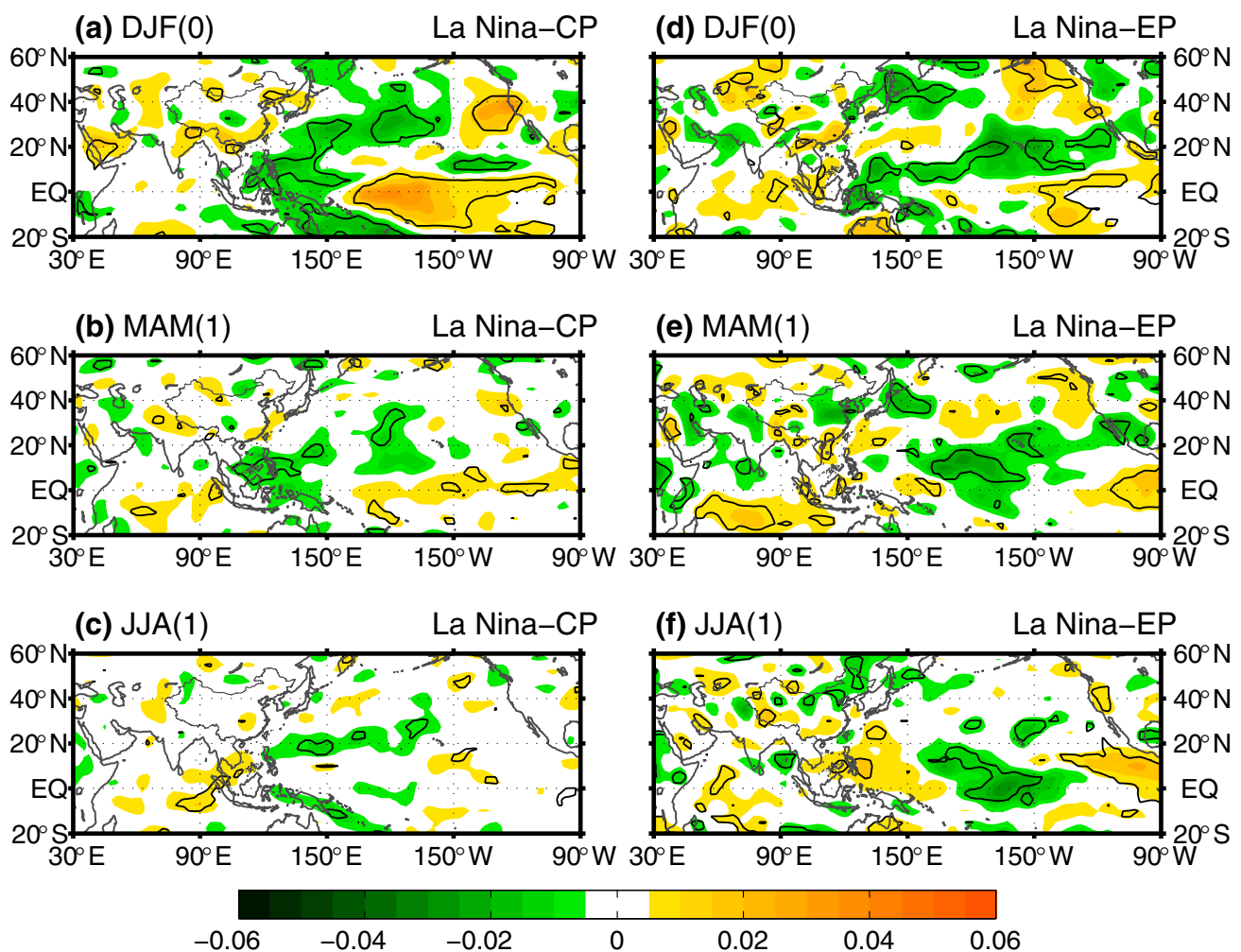


**Fig. 12** Same as Fig. 11, but for **a–c** CP La Niña events and **d–f** EP La Niña events, respectively

**Table 2** List of the experiment design. Note that the GB run, TIOWNP run, TIO run, and WNP run are all forced by the SST anomalies in CP (CP-type experiments) and EP (EP-type experiments) La Niña, respectively

Experiments	Prescribed SST forcing	Integration
CTRL	Monthly climatological SST	20 years
GB run	Add the composite monthly SST anomalies in the global ocean to climatological SST	10 realizations
TIOWNP run	Add the composite monthly SST anomalies in both TIO and WNP to climatological SST	10 realizations
TIO run	Add the composite monthly SST anomalies only in the TIO to climatological SST	10 realizations
WNP run	Add the composite monthly SST anomalies only in the WNP to climatological SST	10 realizations

relative oceanic importance in affecting the WNP circulation anomalies.

Figure 13 illustrates the ensemble-mean 850-hPa wind anomalies in JJA for CP and EP La Niña, respectively. In terms of CP-type experiments, the GB run reproduces the WNPC and the anomalous anticyclone to its north reasonably, with a slight eastward shift of the WNPC (Figs. 7c, 13a). This pattern exists but largely decays in the TIOWNP

run, suggesting the contribution from other oceanic regions (Fig. 13b). The anomalous SST forcing only in TIO stimulates a weak WNPC confined to the SCS (Fig. 13c), consistent with Xie et al. (2009). The superimposed SST anomalies only in WNP excite a weaker and northward WNPC dominant over the WNP region and a cyclone shifting far eastward (Fig. 13d). Therefore, in the case of CP La Niña, the contribution from TIO are more important, which leads

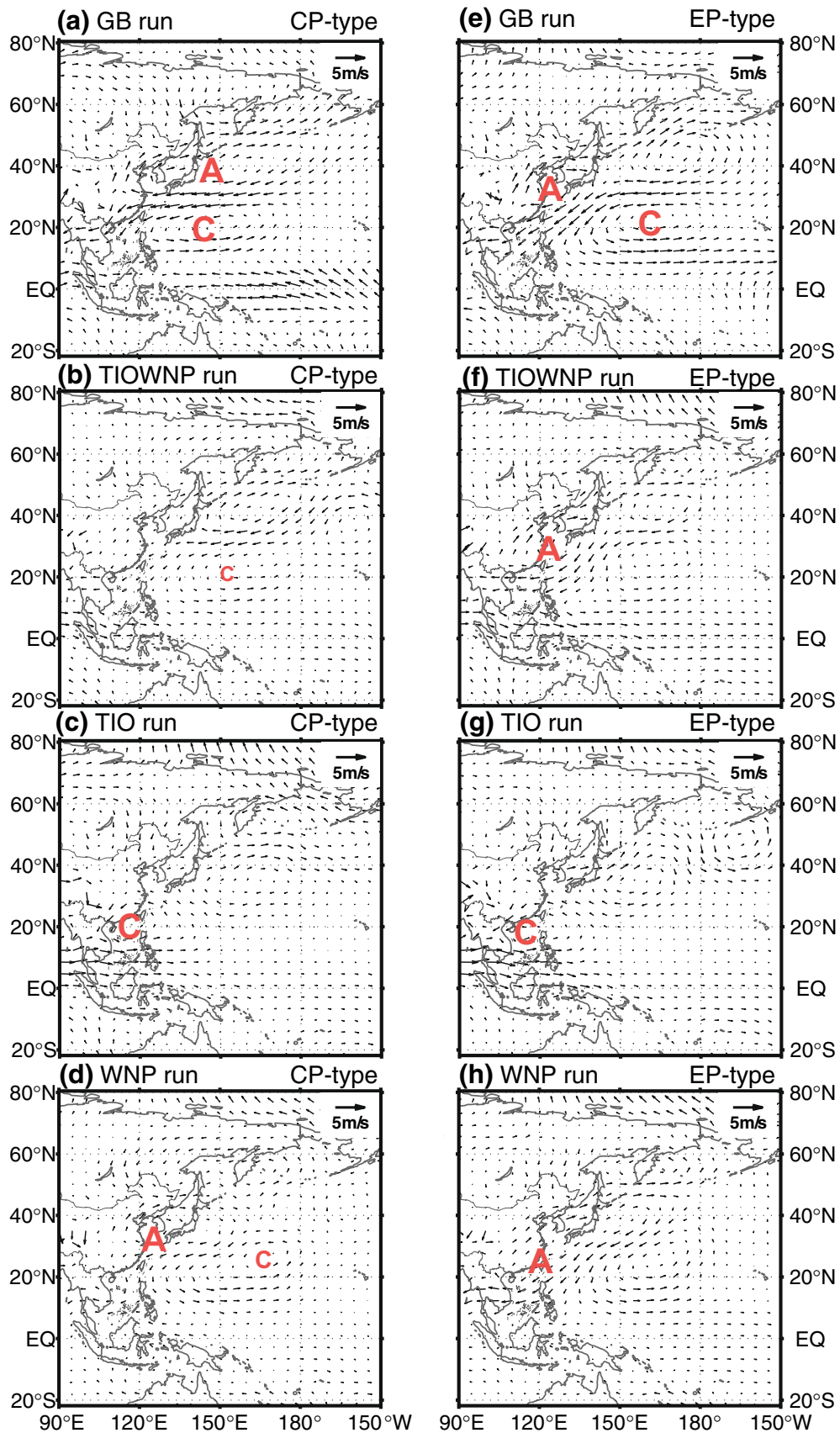




**Fig. 13** The JJA-mean 850-hPa winds (vector) of the ensemble-mean **a** GB run, **b** TIOWNO run, **c** TIO run, and **d** WNP run for CP-type experiments. **e–h** Same as **a–d**, but for EP-type experiments. The red letters “A” and “C” with larger (smaller) size indicate the anticyclonic and cyclonic anomalies with stronger (weaker) intensity, respectively

to the existence of summertime WNPC in its following summer (Figs. 7c, 13a, b). In the aspect of EP-type experiments, a predominant WNPAC emerges and penetrates southward into the SCS in the GB run (Fig. 13e), largely consistent with the observational result (Fig. 7f), but is located northward compared to the observational one. Moreover, the WNPAC also stands out in the EP-type TIOWNP run (Fig. 13f), indicating the crucial role from the key TIO and WNP regions. In EP-type TIO run (Fig. 13g), the pattern with a WNPC over the SCS is very similar to that in CP-type TIO run (Fig. 13c), confirming the role of cooling TIO associated with La Niña events. By contrast, a WNPAC dominates the WNP region in the EP-type WNP run (Fig. 13h) with superimposed cooling SST anomalies only in WNP (Fig. 7d–f). Note that the WNPAC in the WNP run (Fig. 13h) shifts southward compared to those in GB (Fig. 13e) and TIOWNP (Fig. 13f) runs. Thus, the strong cooling over WNP associated with EP La Niña plays a dominant role in affecting the local lower-level circulation aloft.

Further, to quantitatively compare the oceanic contributions in the lower-level circulation over WNP, relative vorticity (RV) anomalies over the region of (8.5°N–35°N, 110°E–150°E) are computed for the ensemble-mean of GB, TIOWNP, TIO, and WNP runs in CP-type and EP-type experiments, respectively (Table 3). In CP-type experiments (Table 3), both GB and TIOWNP runs reproduce the weak WNPC (positive RV anomalies) as denoted in Fig. 7c, with a weaker WNPC in the TIOWNP run, which is in agreement with results in Fig. 13a, b. Moreover, the intensity of WNPC excited in TIO run is stronger than that of the WNPAC (negative RV anomalies) triggered by the local anomalous SST in WNP run, which confirms the larger contribution from TIO in the CP La Niña phenomenon. In view of the EP-type experiments (Table 3), the WNPAC is well simulated in GB and TIOWNP runs. Although a WNPC emerges in TIO run, a much stronger WNPAC is stimulated by the direct SST cooling beneath in WNP run. Hence, the local SST anomalies over WNP play a major role in affecting its circulation anomalies aloft in the summer following EP La Niña events.

## 6 Summary and discussion

### 6.1 Summary

In this study, we have revealed the relationship between EAWM and the ensuing EASM under two types of El Niño

and La Niña events. Results show that the positive (negative) SST anomalies of CP El Niño (La Niña) are mainly located over the CP, while the positive (negative) SST anomalies of EP El Niño (La Niña) largely occupy the EP. In addition, the intensity of EP El Niño (CP La Niña) is stronger than that of CP El Niño (EP La Niña). The CP ENSO is roughly stationary without an obvious propagation but there is an apparent westward propagation for EP ENSO. Above features are mostly consistent with the previous studies (e.g. Ashok et al. 2007; Kug et al. 2009; Feng et al. 2017).

There is an out-of-phase weak EAWM to strong EASM transition when an El Niño event occurs. In detail, the WNPAC can persist from boreal winter to the following spring and summer, bridging the EAWM and EASM. In winter, the southerly flow in the western part of WNPAC weakens the climatological northerly of EAWM and leads to a weak EAWM. Then in boreal summer, the WNPAC is associated with a strong EASM (Fig. 1c). Moreover, the EP El Niño connects a closer EAWM-EASM relationship than that of CP El Niño due to the media of a wider and stronger WNPAC. This difference in WNPAC is caused by both oceanic and atmospheric factors. In the oceanic aspect, the stronger warming over NIO remotely and the more evident dipole (warm in the west and cold in the east) over WNP locally following the EP El Niño contribute to the wider and stronger WNPAC. In the atmospheric aspect, the anomalous sinking branch of Walker Circulation over the WNP acts as a dynamical factor. This vertical motion is stronger and more favorable to the maintenance of WNPAC when EP El Niño occurs. On the La Niña hand, the out-of-phase strong EAWM to weak EASM connection is only observed for CP La Niña in terms of 850-hPa wind anomalies. This connection is much weaker compared to that for two types of El Niño on account of a much weaker WNPC. Although the cooling over NIO and local rising flow should bring a strong WNPC, the local cooling over WNP largely weakens the WNPC in the decaying summer of CP La Niña. Furthermore, the strong EAWM is followed by a strong EASM when EP La Niña occurs, indicating an in-phase transition. The key reason for this in-phase transition is the occurrence of a peculiar WNPAC in summer, originated from the strong cooling and anomalous descending over the WNP locally, with a minor opposite impact from the NIO cooling. Thus, the asymmetry in the EAWM-EASM transition following two types of ENSO events can be attributed to the SST differences in location and intensity and atmospheric dynamical responses consequently.

Numerical simulations of CAM5 validate the above different WNPC/WNPAC evolutions under the CP and EP La Niña. Both GB and TIOWNP runs reproduce the WNP circulation anomalies reasonably for CP-type and EP-type experiments, indicating its robustness associated with La Niña events. In the case of CP La Niña, the contribution

**Table 3** The area-averaged JJA-mean RV anomalies (unit:  $10^{-7} \text{ s}^{-1}$ ) over the region of (8.5°N–35°N, 110°E–150°E) for the ensemble-mean of GB, TIO WNP, TIO, and WNP runs under the associated CP and EP La Niña SST forcing, respectively

	GB run	TIO WNP run	TIO run	WNP run
CP-type experiments	0.57	0.32	1.72	−1.66
EP-type experiments	−1.21	−0.73	1.65	−3.35

from TIO overweighs that from WNP, which induces the summertime WNPC as observed in Fig. 7c. In the aspect of EP-type experiments, the strong cooling over WNP associated with EP La Niña plays a dominant role and triggers the WNPAC aloft. Further, the above circulation anomalies associated with WNPC/WNPAC are confirmed quantitatively from the view of RV anomalies over the WNP region. Overall, the anomalous SST forcing from TIO and WNP plays opposite roles for both CP and EP La Niña events. Specifically, the WNPC dominated by cooling in remote TIO bridges the out-of-phase transition of EAWM and EASM associated with CP La Niña events. On the contrary, the local WNP cooling related to EP La Niña plays a major role in affecting its circulation aloft and induces a WNPAC to connect an in-phase EAWM-EASM relationship.

## 6.2 Discussion

This study acts as a continuation of previous literature associated with the ENSO and EAWM-EASM relationship. Firstly, Chen et al. (2013) elucidated the crucial role of ENSO in this relation, but their linear regression against Niño-3 index cannot separate the ENSO phase (i.e. warm El Niño and cold La Niña conditions) and their types. Further, Xu et al. (2016) investigated the asymmetric role of ENSO in the link between EAWM and following EASM using composite analyses for El Niño and La Niña years. They attributed this asymmetry to the combined effects of oceanic factors from NIO and WNP and atmospheric factors in terms of anomalous vertical motion. Nonetheless, this study did not consider the potential difference in ENSO types (i.e. CP and EP types). For example, Xu et al. (2016) did not explain the reasons for the insignificant circulation anomalies over the WNP in the boreal summer associated with La Niña condition (see their Fig. 2c). Enlightened by above work, we proceed to separate both El Niño and La Niña into CP and EP types and explore their corresponding EAWM-EASM relationship. The replenishment of EAWM-EASM relation under CP and EP La Niña cases is the highlight of this paper. We ascribe the above-mentioned insignificant cyclonic anomalies over the WNP (Fig. 2c in Xu et al. 2016) to the opposite patterns under CP and EP La Niña cases (WNPC in Fig. 7c and WNPAC in Fig. 7f). In the aspect of underlying mechanisms responsible for the WNPAC/WNPC,

the composite analyses reveal the oceanic SST effects from both remote NIO and local WNP and the atmospheric vertical motion using the same approach as in Xu et al. (2016). Moreover, the characteristics of WNPAC during mature and decaying phases of CP and EP El Niño are generally consistent with those derived from the partial correlations against Niño-3 index and EMI in Yuan et al. (2012).

In recent decades, a growing body of evidence proves that the East Asian monsoon is characterized by interdecadal variability, and most studies attribute this interdecadal variability to SST anomalies (e.g. Chang et al. 2000a, b; Wu and Wang 2002; Zhou et al. 2006). Particularly, the connections of ENSO to both EAWM and EASM are modulated by the Pacific decadal oscillation (PDO; Chan and Zhou 2005; Wang et al. 2008a, b). Moreover, the linkage between the EAWM and the EASM is also affected by the PDO (Chen et al. 2013). As shown in Fig. 8, the EAWM-EASM relationship is not stable and only significant in some specific decades even under the influence of ENSO. This may be related to the modulation of PDO and it is yet not clear what specific role the PDO plays in the EAWM-EASM transition under different types and phases of ENSO. In view of the importance of the East Asian monsoon, it is essential to fully expound the role of PDO in the link of EAWM to succeeding EASM associated with different types and phases of ENSO.

**Acknowledgements** We thank Prof. Tim Li at University of Hawaii for his valuable comments and suggestions on this paper. Dr. Chenyu Zhu at Peking University and Dr. Wei Liu at Yale University are acknowledged for great help in model scheme and debugging. Valuable comments from the two anonymous reviewers are highly appreciated. This work is supported by the National Natural Science Foundation of China (41375073 and 41775067).

## References

- An SI, Ham YG, Kug JS, Jin FF, Kang IS (2005) El Niño–La Niña asymmetry in the coupled model intercomparison project simulations. *J Clim* 18(14):2617–2627. <https://doi.org/10.1175/JCLI3433.1>
- Ashok K, Behera SK, Rao SA, Weng H, Yamagata T (2007) El Niño Modoki and its possible teleconnection. *J Geophys Res* 112:C11007. <https://doi.org/10.1029/2006JC003798>
- Burgers G, Stephenson DB (1999) The “normality” of El Niño. *Geophys Res Lett* 26(8):1027–1030. <https://doi.org/10.1029/1999GL900161>
- Cai W, Cowan T (2009) La Niña Modoki impacts Australia autumn rainfall variability. *Geophys Res Lett* 36:L12805
- Chan JC-L, Zhou W (2005) PDO, ENSO and the early summer monsoon rainfall over south China. *Geophys Res Lett* 32:L08810. <https://doi.org/10.1029/2004GL022015>
- Chang CP, Zhang Y, Li T (2000a) Interannual and interdecadal variations of the East Asian summer monsoon and tropical Pacific SSTs. Part I: roles of the subtropical ridge. *J Clim* 13:4310–4325
- Chang CP, Zhang Y, Li T (2000b) Interannual and interdecadal variations of the East Asian summer monsoon and tropical Pacific

- SSTs. Part II: the meridional structure of the monsoon. *J Clim* 13:4326–4340
- Charney J, Shukla J (1981) Predictability of monsoons. In: Lighthill J, Pearce R (eds) *Monsoon dynamics*. Cambridge University Press, Cambridge, pp 99–109
- Chen W (2002) Impacts of El Niño and La Niña on the cycle of the East Asian winter and summer monsoon. *Chin J Atmos Sci* 26(5):595–610. <https://doi.org/10.3878/j.issn.1006-9895.2002.05.02> (Chinese)
- Chen W, Graf HF, Huang RH (2000) The interannual variability of East Asian winter monsoon and its relation to the summer monsoon. *Adv Atmos Sci* 17(1):48–60. <https://doi.org/10.1007/s00376-000-0042-5>
- Chen W, Wang L, Xue Y, Sun S (2009) Variabilities of the spring river runoff system in east China and their relations to precipitation and sea surface temperature. *Int J Climatol* 29:1381–1394. <https://doi.org/10.1002/joc.1785>
- Chen W, Feng J, Wu RG (2013) Roles of ENSO and PDO in the link of the East Asian winter monsoon to the following summer monsoon. *J Clim* 26(2):622–635. <https://doi.org/10.1175/JCLI-D-12-00021.1>
- Chen Y, Hu Q, Yang YM, Qian WH (2017) Anomaly based analysis of extreme heat waves in Eastern China during 1981–2013. *Int J Climatol* 37:509–523
- Chiang JCH, Lintner BR (2005) Mechanisms of remote tropical surface warming during El Niño. *J Clim* 18:4130–4149
- Chiang JCH, Sobel AH (2002) Tropical tropospheric temperature variations caused by ENSO and their influence on the remote tropical climate. *J Clim* 15:2616–2631
- Chou C, Huang LF, Tu J-Y, Tseng L, Hsueh Y-C (2009) El Niño impacts on precipitation in the western North Pacific–East Asian sector. *J Clim* 22:2039–2057
- Deser C, Alexander MA, Xie SP, Phillips AS (2010) Sea surface temperature variability: patterns and mechanisms. *Annu Rev Marine Sci* 2:115–143. <https://doi.org/10.1146/annurevmarine-120408-151453>
- Ding YH (1992) Summer monsoon rainfalls in China. *J Meteorol Soc Jpn* 70:373–396
- Ding YH (1994) *Monsoon over China*. Kluwer Academic, Dordrecht, p 420
- Dommenget D, Bayr T, Frauen C (2013) Analysis of the non-linearity in the pattern and time evolution of El Niño southern oscillation. *Clim Dyn* 40:2825–2847
- Du Y, Xie SP, Huang G, Hu KM (2009) Role of air–sea interaction in the long persistence of El Niño-induced North Indian Ocean warming. *J Clim* 22:2023–2038
- Feng J, Chen W, Li YJ (2017) Asymmetry of the winter extra-tropical teleconnections in the Northern Hemisphere associated with two types of ENSO. *Clim Dyn* 48:2135–2151
- Frauen C, Dommenget D, Tyrrell N, Rezny M, Wales S (2014) Analysis of the nonlinearity of El Niño–Southern Oscillation teleconnections. *J Clim* 27:6225–6244
- Gill AE (1980) Some simple solutions for heat-induced tropical circulation. *Q J R Meteorol Soc* 106:447–462. <https://doi.org/10.1002/qj.49710644905>
- Hoerling MP, Kumar A, Zhong M (1997) El Niño, La Niña, and the nonlinearity of their teleconnections. *J Clim* 10(8):1769–1786. [https://doi.org/10.1175/1520-0442\(1997\)010<1769:ENOLNA>2.0.CO;2](https://doi.org/10.1175/1520-0442(1997)010<1769:ENOLNA>2.0.CO;2)
- Hsu HH, Weng CH (2001) Northwestward propagation of the intraseasonal oscillation in the western North Pacific during boreal summer: structure and mechanism. *J Clim* 14:3834–3850
- Huang RH, Zhou LT, Chen W (2003) The progresses of recent studies on the variabilities of the East Asian monsoon and their causes. *Adv Atmos Sci* 20:55–69
- Huang RH, Chen JL, Huang G (2007) Characteristics and variations of the East Asian monsoon system and its impacts on climate disasters in China. *Adv Atmos Sci* 24:993–1023. <https://doi.org/10.1007/s00376-007-0993-x>
- Hurrell JW, Hack JJ, Shea D (2008) A new sea surface temperature and sea ice boundary dataset for the community atmosphere model. *J Clim* 21:5145–5153
- Jin FF, An SI, Timmermann A, Zhao JX (2003) Strong El Niño events and nonlinear dynamical heating. *Geophys Res Lett* 30(3):1120. <https://doi.org/10.1029/2002GL016356>
- Kalnay E et al (1996) The NCEP/NCAR 40-year reanalysis project. *Bull Am Meteorol Soc* 77: 437–471. [https://doi.org/10.1175/1520-0477\(1996\)077<0437:TNYRP.2.0.CO;2](https://doi.org/10.1175/1520-0477(1996)077<0437:TNYRP.2.0.CO;2)
- Kang IS, Kug JS (2002) El Niño and La Niña sea surface temperature anomalies: asymmetry characteristics associated with their wind stress anomalies. *J Geophys Res* 107(19):4372. <https://doi.org/10.1029/2001JD000393>
- Kao HY, Yu JY (2009) Contrasting eastern-Pacific and central-Pacific types of ENSO. *J Clim* 22:615–632
- Kim HM, Webster PJ, Curry JA (2011) Modulation of North Pacific tropical cyclone activity by three phases of ENSO. *J Clim* 24:1839–1849
- Kug JS, Jin FF, An SI (2009) Two types of El Niño events: cold tongue El Niño and warm pool El Niño. *J Clim* 22:1499–1515. <https://doi.org/10.1175/2008JCLI2624.1>
- Larkin NK, Harrison DE (2005) Global seasonal temperature and precipitation anomalies during El Niño autumn and winter. *Geophys Res Lett* 32:L16705. <https://doi.org/10.1029/2005GL022860>
- Lau KM (1992) East Asian summer monsoon rainfall variability and climate teleconnection. *J Meteorol Soc Japan* 70:211–242
- Lau KM, Li MT (1984) The monsoon of East Asia and its global associations—A survey. *Bull Am Meteorol Soc* 65(2):114–125. [https://doi.org/10.1175/1520-0477\(1984\)065<0114:TMOEAA>2.0.CO;2](https://doi.org/10.1175/1520-0477(1984)065<0114:TMOEAA>2.0.CO;2)
- Lau KM, Yang GJ, Shen SH (1988) Seasonal and intraseasonal climatology of summer monsoon rainfall over East Asia. *Mon Weather Rev* 116:18–37
- Li CY, Pan J, Que ZP (2011) Variation of the East Asian monsoon and the tropospheric biennial oscillation. *Chin Sci Bull* 56(1):70–75. <https://doi.org/10.1007/s11434-010-4200-6>
- Neelin JD, Battisti DS, Hirst AC, Jin FF, Wakata Y, Yamagata T, Zebiak SE (1998) ENSO theory. *J Geophys Res* 103:14261–14290
- Peng JB, Zhang QY, Bueh C (2007) On the characteristics and possible causes of a severe drought and heat wave in the Sichuan-Chongqing region in 2006. *Clim Environ Res* 12(3):464–474 (Chinese)
- Qian WH, Shi J (2017) Tripole precipitation pattern and SST variations linked with extreme zonal activities of the western Pacific subtropical high. *Int J Climatol* 37(6):3018–3035
- Rayner NA, Parker DE, Horton EB, Folland CK, Alexander LV, Rowell DP, Kent EC, Kaplan A (2003) Global analyses of sea surface temperature, sea ice, and night marine air temperature since the late nineteenth century. *J Geophys Res* 108:4407. <https://doi.org/10.1029/2002JD002670>
- Ren HL, Jin FF (2011) Niño indices for two types of ENSO. *Geophys Res Lett* 38:L04704. <https://doi.org/10.1029/2010GL046031>
- Reynolds RW, Smith TM (1994) Improved global sea surface temperature analyses using optimum interpolation. *J Clim* 7:929–948
- Saji NH, Xie SP, Yamagata T (2006) Tropical Indian Ocean variability in the IPCC 20th-century climate simulations. *J Clim* 19:4397–4417
- Shinoda T, Hurlburt HE, Metzger EJ (2013) Anomalous tropical ocean circulation associated with La Niña Modoki. *J Geophys Res* 116:C12001. <https://doi.org/10.1029/2011JC007304>
- Song LY, Chen SF, Chen W, Chen XL (2017) Distinct impacts of two types of La Niña events on Australian summer rainfall. *Int J Climatol* 37:2532–2544

- Sun BM, Sun SQ (1994) The analysis on the features of the atmospheric circulation in preceding winters for the summer drought and flooding in the Yangtze and Huaihe River valley. *Adv Atmos Sci* 11:79–90
- Sun SQ, Sun BM (1995) The relationship between the anomalous winter monsoon circulation over East Asia and summer drought/flooding in the Yangtze and Huaihe River valley. *Chin J Atmos Sci* 53(4):440–450 (Chinese)
- Sun Y, Zhang XB, Zwiers FW, Song LC, Wan H, Hu T, Yin H, Ren GY (2014) Rapid increase in the risk of extreme summer heat in Eastern China. *Nat Clim Change* 4:1082–1085
- Tao SY, Chen LX (1987) A review of recent research on the East Asian summer monsoon in China. Chang CP, Krishnamurti TN (eds) *Monsoon Meteorology*. Oxford University Press, Oxford, pp 60–92
- Trenberth KE, Hurrell JW, Stepaniak DP (2006) The Asian monsoon: global perspectives. *The Asian Monsoon*. Wang B (ed) Springer, Berlin, pp 67–87
- Wang B, Fan Z (1999) Choice of South Asian summer monsoon indices. *Bull Am Meteor Soc* 80:629–638
- Wang X, Wang C (2014) Different impacts of various El Niño events on the Indian Ocean Dipole. *Clim Dyn* 42:991–1005
- Wang L, Wu RG (2012) In-phase transition from the winter monsoon to the summer monsoon over East Asia: role of the Indian Ocean. *J Geophys Res Atmos* 117(D11):11112
- Wang B, Zhang Q (2002) Pacific–East Asian teleconnection. Part II: How the Philippine Sea anomalous anticyclone is established during El Niño development? *J Clim* 15:3252–3265
- Wang QL, Zhang LF (2008) Circulation characteristics of high temperature and drought in summer of 2006 in Chongqing. *Arid Meteorol* 26(1):1–7 (Chinese)
- Wang B, Wu RG, Fu XH (2000) Pacific–East Asian teleconnection: How does ENSO affect East Asian climate? *J Clim* 13:1517–1536
- Wang B, Wu ZW, Li JP, Liu J, Chang C-P, Ding YH, Wu GX (2008a) How to measure the strength of the East Asian summer monsoon. *J Clim* 21(17):4449–4463
- Wang L, Chen W, Huang RH (2008b) Interdecadal modulation of PDO on the impact of ENSO on the East Asian winter monsoon. *Geophys Res Lett* 35:L20702. <https://doi.org/10.1029/2008GL035287>
- Watanabe M, Jin FF (2002) Role of Indian Ocean warming in the development of Philippine Sea anticyclone during ENSO. *Geophys Res Lett* 29:1478. <https://doi.org/10.1029/2001GL014318>
- Weng H, Ashok K, Behera SK, Rao SA (2007) Impacts of recent El Niño Modoki on dry/wet conditions in the Pacific Rim during boreal summer. *Clim Dyn* 29:113–129
- Wu RG (2010) Subseasonal variability during the South China Sea summer monsoon onset. *Clim Dyn* 34:629–642. <https://doi.org/10.1007/s00382-009-0679-4>
- Wu AM, Ni YQ (1997) The influence of Tibetan Plateau on the interannual variability of Asian monsoon. *Adv Atmos Sci* 14:491–504
- Wu RG, Wang B (2002) A contrast of the East Asian summer monsoon and ENSO relationship between 1962–77 and 1978–93. *J Clim* 15:3266–3279
- Wu B, Zhou TJ, Li T (2009) Seasonally evolving dominant interannual variability modes of East Asian climate. *J Clim* 22:2992–3005
- Wu B, Li T, Zhou TJ (2010) Relative contributions of the Indian Ocean and local SST anomalies to the maintenance of the western North Pacific anomalous anticyclone during El Niño decaying summer. *J Clim* 23:2974–2986
- Xie SP, Hu KM, Hafner J, Tokinaga H, Du Y, Huang G, Sampe T (2009) Indian Ocean capacitor effect on Indo-western Pacific climate during the summer following El Niño. *J Clim* 22:730–747
- Xu PQ, Feng J, Chen W (2016) Asymmetric role of ENSO in the link between the East Asian winter monsoon and the following summer monsoon. *Chin J Atmos Sci* 40(4):831–840 (Chinese)
- Yan HM, Duan W, Xiao ZN (2003) A study on relation between East Asian winter monsoon and climate change during raining season in China. *J Trop Meteorol* 19(4):367–376
- Yan HM, Yang H, Yuan Y, Li CY (2011) Relationship between East Asian winter monsoon and summer monsoon. *Adv Atmos Sci* 28:1345–1356
- Yang S, Lau KM, Kim KM (2002) Variations of the East Asian jet stream and Asian–Pacific–American winter climate anomalies. *J Clim* 15:306–325
- Yang JL, Liu QY, Xie SP, Liu ZY, Wu LX (2007) Impact of the Indian Ocean SST basin mode on the Asian summer monsoon. *Geophys Res Lett* 34:L02708. <https://doi.org/10.1029/2006GL028571>
- Yu JY, Kao HY (2007) Decadal changes of ENSO persistence barrier in SST and ocean heat content indices: 1958–2001. *J Geophys Res* 112:D13106. <https://doi.org/10.1029/2006JD007654>
- Yu JY, Kim ST (2011) Relationship between extratropical sea level pressure variations and the central Pacific and eastern Pacific types of ENSO. *J Clim* 24:708–720
- Yuan Y, Yan HM (2013) Different types of La Niña events and different responses of the tropical atmosphere. *Chin Sci Bull* 58:406–415. <https://doi.org/10.1007/s11434-012-5423-5>
- Yuan Y, Yang S, Zhang ZQ (2012) Different evolutions of the Philippine Sea anticyclone between the Eastern and Central Pacific El Niño: possible effects of Indian Ocean SST. *J Clim* 25(22):7867–7883
- Zhang RH, Sumi A, Kimoto M (1996) Impact of El Niño on the East Asian monsoon: a diagnostic study of the '86/87 and '91/92 events. *J Meteorol Soc Jpn* 74:49–62
- Zhang RH, Sumi A, Kimoto M (1999) A diagnostic study of the impact of El Niño on the precipitation in China. *Adv Atmos Sci* 16:229–241
- Zhang WJ, Jin FF, Zhao JX, Qi L, Ren HL (2013) The possible influence of a nonconventional El Niño on the severe autumn drought of 2009 in southwest China. *J Clim* 26:8392–8405
- Zhang T, Perlwitz J, Hoerling MP (2014) What is responsible for the strong observed asymmetry in teleconnections between El Niño and La Niña? *Geophys Res Lett* 41:1019–1025
- Zhang RH, Li TR, Wen M, Liu L (2015a) Role of intraseasonal oscillation in asymmetric impacts of El Niño and La Niña on the rainfall over southern China in boreal winter. *Clim Dyn* 45:559–567
- Zhang WJ, Wang L, Xiang BQ, Qi L, He JH (2015b) Impacts of two types of La Niña on the NAO during boreal winter. *Clim Dyn* 44:1351–1366. <https://doi.org/10.1007/s00382-014-2155-z>
- Zhou W, Chan JC-L, Li CY (2005) South China Sea summer monsoon onset in relation to the off-equatorial ITCZ. *Adv Atmos Sci* 22:665–676
- Zhou W, Li CY, Chan JC-L (2006) The interdecadal variations of the summer monsoon rainfall over south China. *Meteorol Atmos Phys* 93:165–175. <https://doi.org/10.1007/s00703-006-0184-9>